JOURNAL OF NEUROTRAUMA 36:3138–3157 (November 15, 2019)
Mary Ann Liebert, Inc.
DOI: 10.1089/neu.2019.6423

Exposure to Blast Overpressure Impairs Cerebral Microvascular Responses and Alters Vascular and Astrocytic Structure

Rania Abutarboush,[1,4] Ming Gu,[1,4] Usmah Kawoos,[1,4] Saad H. Mullah,[1,4] Ye Chen,[1,4] Samantha Y. Goodrich,[1,4] Margaret Lashof-Sullivan,[1,4] Richard M. McCarron,[1,5] Jonathan K. Statz,[1,4] Randy S. Bell,[2] James R. Stone,[3] and Stephen T. Ahlers[1]

Abstract

Exposure to blast overpressure may result in cerebrovascular impairment, including cerebral vasospasm. The mechanisms contributing to this vascular response are unclear. The aim of this study was to evaluate the relationship between blast and functional alterations of the cerebral microcirculation and to investigate potential underlying changes in vascular microstructure. Cerebrovascular responses were assessed in sham- and blast-exposed male rats at multiple time points from 2 h through 28 days after a single 130-kPa (18.9-psi) exposure. Pial microcirculation was assessed through a cranial window created in the parietal bone of anesthetized rats. Pial arteriolar reactivity was evaluated *in vivo* using hypercapnia, barium chloride, and serotonin. We found that exposure to blast leads to impairment of arteriolar reactivity >24 h after blast exposure, suggesting delayed injury mechanisms that are not simply attributed to direct mechanical deformation. Observed vascular impairment included a reduction in hypercapnia-induced vasodilation, increase in barium-induced constriction, and reversal of the serotonin effect from constriction to dilation. A reduction in vascular smooth muscle contractile proteins consistent with vascular wall proliferation was observed, as well as delayed reduction in nitric oxide synthase and increase in endothelin-1 B receptors, mainly in astrocytes. Collectively, the data show that exposure to blast results in delayed and prolonged alterations in cerebrovascular reactivity that are associated with changes in the microarchitecture of the vessel wall and astrocytes. These changes may contribute to long-term pathologies involving dysfunction of the neurovascular unit, including cerebral vasospasm.

Keywords: blast overpressure; cerebrovascular reactivity; *in vivo* studies; microcirculation; vascular injury

Introduction

Exposure to blast overpressure (BOP) from high-energy explosions has been on the rise in the civilian population and combat troops. A notable clinical finding in military casualties exposed to blast is cerebral vasospasm, a complication experienced more commonly by blast casualties than other forms of traumatic brain injury (TBI).[1] Post-traumatic vasospasm is a delayed, highly unpredictable pathological phenomenon, often occurring in brain regions distal from the primary site of injury and is most commonly associated with the presence of subarachnoid hemorrhage (SAH). Significant constriction of the lumen of major cerebral arteries and diminished blood flow occur 3–7 days post-SAH,[2] with earlier onset in blast-induced TBI.[1] A seminal study by Armonda and colleagues[3] found that nearly half of 57 patients with severe blast-induced TBI suffered from angiographic cerebral vasospasm, which tended to peak 14–16 days post-injury and was observed up to 30 days after the initial traumatic insult. Of note, blast exposure was sufficient to initiate vasospasm in the absence of SAH. The presence of vasospasm alone predicted negative short- and long-term clinical outcomes. Though the underlying pathophysiology is unclear, the presence of vasospasm

[1]Neurotrauma Department, Naval Medical Research Center, Silver Spring, Maryland.
[2]Neurosurgery Department, Walter Reed National Military Medical Center, Bethesda, Maryland.
[3]Department of Radiology and Medical Imaging, University of Virginia Medical Center, Charlottesville, Virginia.
[4]The Henry M. Jackson Foundation for the Advancement of Military Medicine Inc., Bethesda, Maryland.
[5]Department of Surgery, Uniformed Services University of the Health Sciences, Bethesda, Maryland.

in the absence of SAH suggests unique mechanisms from non-blast TBI.

Cerebrovascular injury remains a poorly studied pathogenic mechanism in blast-induced TBI, particularly in mild cases that rarely come to autopsy.[4] Converging lines of evidence suggest that blast exposure is associated with vascular pathology. Experimentally, blast TBI is associated with alterations in blood–brain barrier (BBB) permeability,[5–7] cerebral perfusion,[8] and autoregulation.[9] Repeated exposure to blast results in a uniform degradation of the cerebral endothelial glycocalyx with pervasive small vessel pathology,[10] and long-term vascular pathology has been reported in the absence of overt neuronal damage.[11,12] Additionally, exposure to blast impairs the vasodilatory ability of the basilar artery *ex vivo*[13] and increases vascular smooth muscle contractility *in vitro*.[14]

Despite clinical indications and experimental data supporting a role of cerebrovascular insult in the pathogenesis of blast-induced TBI, there remains a paucity of data on alterations in microvascular structure and function after exposure to blast. Various physiological mechanisms regulate the cerebral microcirculation to produce vasodilation or vasoconstriction,[15] and the balanced responses of the cerebral vasculature are critical for neurovascular coupling, maintaining constant blood flow by autoregulatory mechanisms, and responding to neurohumoral stimuli. Changes in cerebrovascular reactivity are predictive of SAH-induced vasospasm.[16] Evidence of vascular damage in cerebral vasospasm comes from the spontaneous activity of vascular smooth muscle resulting in vasoconstriction in the early phase. Subsequent proliferation of these cells leads to vascular wall thickening, changes in arterial compliance, and resistance to treatment with vasodilator pharmacological agents.[2,17–19] Increase in arterial rigidity caused by injury to the vascular endothelium and smooth muscle is a well-established concept in cardiovascular disease,[20] where contractile vascular smooth cells switch to a pro-proliferative, non-contractile phenotype in response to changes in intravascular mechanical forces, resulting in vascular remodeling.

The unique mechanics of blast and the response of the cerebral vasculature to rapid acute increase in pressure loads may contribute to alterations in cerebrovascular reactivity, vascular remodeling, and initiation of vasospasm. Indeed, *in vitro* and *ex vivo* studies suggest that exposure to blast may be associated with vascular remodeling and altered vasoreactivity.[13,14] Therefore, our study sought to assess blast-induced changes in pial microvascular responsiveness to mechanistically varied vasoactive mediators *in vivo*, characterize the time course of any observed microvascular dysfunction, and examine structural changes in the vasculature within the same time frame. Our data indicate that blast exposure is associated with impaired microvascular dilation and enhanced constriction, along with alterations in vascular smooth muscle, the endothelium, and astrocytes.

Methods

The study protocol was reviewed and approved by the Walter Reed Army Institute of Research/Naval Medical Research Center Institutional Animal Care and Use Committee in compliance with all applicable federal regulations governing the protection of animals in research.

Blast overpressure exposure

Anesthetized male, 7–9 weeks old, hooded Long Evans rats (Charles River Laboratories, Wilmington, MA), weighing 357 ± 4 g, were exposed to blast overpressure in a compressed air-driven shock tube as previously described.[21,22] Mylar sheets (DuPont Co., Wilmington, DE), 350 μm thick, were used to separate the compression and expansion chambers in the tube to generate a blast wave with a mean peak pressure of 130 ± 0.61 kPa (mean ± standard error of the mean [SEM]; equivalent to ~18.9 psi), overpressure duration of 9.26 ± 0.21 ms (mean ± SEM), and overpressure impulse of 510 ± 0.004 kPa.ms (mean ± SEM). Under 4% isoflurane anesthesia, each rat was placed in a plastic cone (DeCapi Cones; BrainTree Scientific Inc., Braintree, MA) to restrain head and body movements induced by the shock wave. The rat was then placed under three rubber tourniquets in an animal holding basket inside the shock tube to further stabilize the head, chest, and lower torso during blast exposure. All rats were exposed to a single blast in the frontal facing position (i.e., nose and head 180 degrees relative to the pressure wave propagation. Sham (non-blast) rats were exposed to all procedures but the blast.

After blast exposure, rats were allowed to recover from anesthesia and returned to their cages until the appropriate study time point. For intravital microscopy studies, rats were randomized into 2 h, 1, 3, 14, or 28 days post-BOP groups before exposure to blast. For immunohistochemistry (IHC) and western blot studies, a randomized block design was used. Because of the large number of animals needed to complete the studies reported here, only male rats were used in this initial investigation to control for sex-related differences. The majority of reports of clinical outcome after exposure to blast are based on observations in male military service members attributed to higher participation and incidence of injury in males.[23,24] The findings of our study are limited to males, and sex differences in cerebrovascular responsiveness after exposure to blast remain unknown. It will be crucial that future studies investigate the effects in females.

Intravital microscopy: pial arteriolar reactivity

After exposure to sham procedures or BOP and on the day of surgery, rats were weighed and anesthetized with an intraperitoneal injection of a mixture of acepromazine (4 mg/kg) and ketamine (72 mg/kg). Buprenorphine (0.01 mg/kg) was administered subcutaneously for analgesia. Surgical plane of anesthesia was maintained subsequently with intramuscular injections of ketamine. Throughout the study, core body temperature was maintained at 37°C with a warming pad (MouseVent; Kent Scientific, Lichtfield, CT). Because pilot studies showed that rats breathing room air (21% oxygen) became hypoxemic, all animals were mechanically ventilated by an endotracheal tube with a small animal ventilator (MouseVent) using 40% medical grade oxygen (O_2) and 60% nitrogen (N_2; Airgas, Alexandria, VA). Ventilator settings were adjusted to maintain normocapnia (partial pressures of carbon dioxide [p_aCO_2] of 35–45 mm Hg) and normoxia (partial pressures of oxygen [p_aO_2] ≥80 mm Hg).

The right femoral artery was cannulated with PE-50 tubing for continuous blood sampling and invasive arterial blood pressure and heart rate (HR) monitoring (MouseVent). Blood samples were analyzed on an automated blood-gas system (ABL 700; Radiometer Medical ApS, Copenhagen, Denmark) for pH, p_aCO_2, and p_aO_2, lactate, and bicarbonate (HCO_3^-). Pial microcirculation was accessed through a rectangular craniotomy (~3 × 4 mm) prepared in the right parietal bone as described in Levasseur and colleagues.[25] The dura was cut and removed to the side to expose pial microvasculature. To maintain moisture and electrolyte balance, the surface of the brain was superfused with artificial cerebrospinal fluid (CSF; Na 150 mM, K 3.0 mM, Ca 1.4 mM, Mg 0.8 mM, P 1.0 mM, and Cl 155 mM; Harvard Apparatus, Holliston, MA) and covered with a glass cover-slip. A stereomicroscope (SZ16; Olympus, Tokyo, Japan) equipped with a DP-73 digital camera was used for imaging pial microvessels. A total magnification of 40× and a resolution of 0.8063 pixel/micrometer for both X and Y

dimensions were used for image collection. Pial arterioles were measured at the same locus throughout the experiment using the computer program CellSens (2010; Olympus).

After a 10-min stabilization period after surgery and under anesthesia, vessel reactivity was assessed by measuring pial arteriolar diameters before and after treatment with each of three mechanistically varied vasoactive mediators: carbon dioxide (CO_2), barium chloride ($BaCl_2$), and serotonin (5-hydroxytryptamine; 5-HT). The vasodilatory response of CO_2 was assessed by switching the ventilator air supply from 40% O_2 to a certified gas mixture of 7% CO_2, 40% O_2, and 53% N_2 (Airgas). The CO_2 test was terminated when end-tidal CO_2 readings reached 10%, which typically occurred after $\sim$90 sec. An arterial blood-gas sample was analyzed at the end of the CO_2 test to confirm that p_aCO_2 increased to at least $\sim$70 mm Hg. After a 10-min washout period with artificial CSF, 5% aqueous $BaCl_2$ (0.3 mL) was applied topically to the pia dropwise to probe vascular reactivity to this potent vasoconstrictor.[26,27]

For the 5-HT response, 0.3 mL of 1×10^{-4} M of 5-HT HCl (Sigma-Aldrich, St Louis, MO) was applied topically to the pial surface after a 10-min washout period with artificial CSF after the $BaCl_2$ test. At the end of the experiment, reactivity of the pial microcirculation was tested again with $BaCl_2$ and CO_2 to ensure that the vessels remained reactive and able to constrict or dilate, respectively, until the end of the experiment. Figure 1 illustrates examples of vasoconstriction and -dilation of pial arterioles as seen through a cranial window.

For analysis of microvascular diameter changes, pial microvessels were grouped into either a ''small'' (<50 μm) or ''medium'' (50–100 μm) size category based on the pre-treatment baseline size.[28–35] The increase in the amount of smooth muscle with vessel size correlates with the ability of vessels to contract justifies dividing the vessels into size categories.[27] A power analysis of pilot data indicated that 40 vessels per size category were required to detect a 10% change in diameter with 80% power. All animals were euthanized with 150 mg/kg of sodium pentobarbital at the end of the experiment administered by intracardiac puncture.

Immunohistochemistry

To characterize blast-induced changes within the vascular wall and astrocytes and the time course of these changes, the expression of the following proteins was examined using IHC: vascular smooth muscle protein smoothelin (SMTH), smooth muscle α-actin (SMA), smooth muscle myosin heavy chain (SM-MHC), myosin light chain II-20 kDa (MLC), endothelin type A receptor (ET_A), endothelin type B receptor (ET_B), and the astrocyte marker glial fibrillary acidic protein (GFAP). Rats were exposed to BOP or sham procedures as described above, and, at each of the time points studied (2 h and 1, 3, 14, and 28 days post-BOP), rats ($n=5$ rats/group for each time point) were euthanized with sodium pentobarbital (150 mg/kg) and brains were collected and immediately embedded in optimal cutting temperature compound (Sakura Finetek, Torrance, CA) on dry ice.

Frozen cryostat sections (5 μm) from 0.8 mm anterior to bregma to 4.8 mm posterior to bregma were washed in phosphate-buffered saline (PBS) for 15 min and blocked in 2% bovine serum albumin in PBS for 30 min at room temperature. Sections were then incubated with rabbit or mouse antibodies against SMTH (1:2000; Invitrogen, Carlsbad, CA), SMA (1:500; Santa Cruz Biotechnology, Santa Cruz, CA), SM-MHC (1:500; Invitrogen), MLC (1:500; Cell Signaling Technologies, Danvers, MA), ET_A (1:500; Abcam, Cambridge, UK), ET_B (1:500; Abcam), or GFAP (1:1000; Millipore, Burlington, MA) overnight at 4°C. After three washes in PBS, the sections were incubated with the appropriate cyanine (Cy) 2– or Cy3-conjugated secondary antibodies (1:500; Jackson ImmunoResearch, West Grove, PA) at room temperature or overnight at 4°C. Sections were then washed in PBS, dehydrated through a graded (50, 70, 80, 90, and 100%) series of water-ethanol, cleared with xylene, mounted with Permount, and cover-slipped. For all proteins, with the exception of the endothelin receptors, sections were examined with an Olympus AX80 (Olympus) and images were captured with a DP72 camera (Olympus) using the software, cellSens Dimension (Olympus).

Immunofluorescence intensity, blood vessel thickness, and vessel luminal diameter were measured using the software, ImagePro Premier (Version 9.3; Media Cybernetics Inc., Rockville, MD). Images from six to eight sections from each animal were used for semiquantitative analyses. For analysis of SMTH, SMA, SM-MHC, and MLC immunostained sections, the threshold was adjusted so that only the fluorescent staining (and not the background) was visible. Image color was converted to black and white, with white representing the immunostained areas and black representing non-stained areas. For consistency, the same threshold was applied to all sections. Individual vessels were selected, and densitometry of immunolabeled vessels was used to obtain intensity values.

To determine whether exposure to blast leads to change in expression pattern of endothelin receptors within the blood vessel wall and astrocytes, tissue sections were double-labeled against endothelin receptors A or B and GFAP or SMA to label astrocytes or smooth muscle, respectively. For colocalization studies, the same standard immunolabeling procedures described above were used and the sections that were incubated with anti-ET_A or ET_B antibodies were combined with anti-SMA or anti-GFAP antibodies. Immunofluorescence was examined using confocal microscopy (Fluoview FV1200; Olympus). For quantification of ET receptors, single immunofluorescence intensity for the whole slide was obtained. Double-labeled cells were counted manually and were

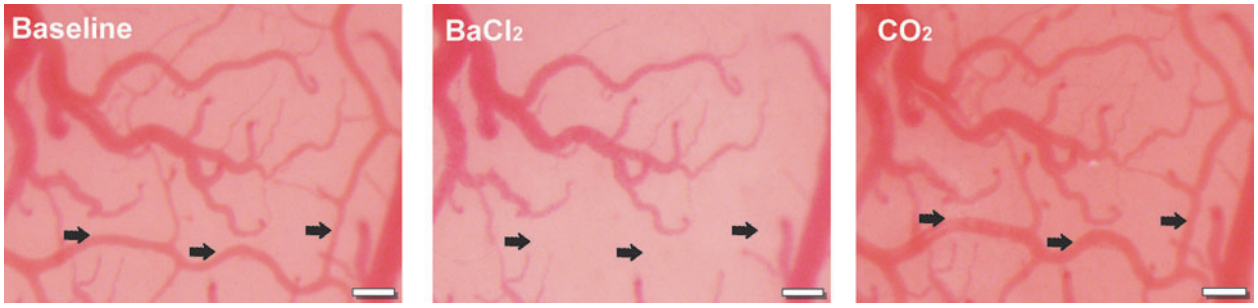

FIG 1. An example of pial microcirculation as seen through a cranial window in the parietal bone under baseline conditions (left, $p_aCO_2=35$–45 mm Hg), after topical application of $BaCl_2$ (middle, $p_aCO_2=35$–45 mm Hg), and after ventilation with 7% CO_2 (right, $p_aCO_2=80.6$ mm Hg in the illustrated example). Pial arterioles (arrows) respond with vasoconstriction to $BaCl_2$ and $\sim$4% dilation to 7% CO_2. Scale bars, 100 μm. p_aCO_2, partial pressure of carbon dioxide.

expressed as percentage of ET_A or ET_B and GFAP-positive cells or ET_A or ET_B and SMA-positive cells.

Western blotting

For western blotting, anesthetized rats ($n = 6$ rats/group for each time point) were exposed to blast or sham procedures and euthanized as described for IHC. Harvested brains were flash-frozen in liquid nitrogen until further processing. For protein extraction, tissue from the frontoparietal cortex was sonicated and lysed on ice in a buffer containing 150 mM of NaCl, 50 mM of Tris-HCl, 0.25% deoxycholate, 1 mM of ethylene glycol tetraacetic acid, 1 mM of NaF, 1 mM of Na_3VO_4, and a cocktail of proteinase inhibitors. Protein assays and western blot analyses were determined as previously described.[36] Briefly, equal amounts of protein from each sample (25 μg) were subjected to sodium dodecyl sulfate polyacrylamide gel electrophoresis and transferred to polyvinylidene difluoride membranes, which were then blocked in 5% nonfat milk. Membranes were then probed overnight at 4°C using the following dilutions of the same antibodies used for IHC: SMTH (1:2500), SM-MHC (1:1000), SMA (1:1000), MLC (1:1000), ET_A (1:1000), and ET_B (1:2000).

In addition, antibodies against endothelin-1 (ET-1; 1:1000; Invitrogen), endothelial nitric oxide synthase (eNOS; 1:1000; Abcam), inducible nitric oxide synthase (iNOS; 1:1000; Thermo Fisher Scientific, Waltham, MA), and serine 19 phosphorylated MLC (p-MLC; 1:1000; Cell Signaling) were also used to assess expression of these proteins. After incubation with the appropriate antimouse or -rabbit secondary horseradish peroxidase (HRP)-linked immunoglobulin G secondary antibodies (Cell Signaling), blots were developed with an enhanced chemiluminescence reagent (SuperSignal WestFemto; Thermo Fisher Scientific) and imaged in a Fuji Image analyzer (LAS-3000; Fujifilm, Tokyo, Japan) to detect the HRP-conjugated antibody complex. Band density was quantified using the NIH software, ImageJ (NIH, Bethesda, MD). Each membrane was then incubated in a stripping buffer for 15 min to remove the immune complex and probed for the housekeeping protein, β-actin.

Statistical analysis

All results are reported as mean ± SEM. Statistical analyses were performed using SPSS software (2012; IBM Corporation, Armonk, NY). Data for each variable were assessed for normality before inferential statistical analyses. For pial arteriolar diameters, percent change from pre-treatment baseline for each vasoactive mediator was compared among the groups using the Mann-Whitney U test because the data were not normally distributed and a transformation was not feasible. Adjustments for multiple comparisons against the sham group were performed, and, when appropriate, the adjusted p values were used to determine statistical significance. GraphPad Prism software (version 6; 2009; GraphPad Software Inc., San Diego, CA) was used for generating graphs. IHC and western blotting data were analyzed using analysis of variance (ANOVA), followed by Dunnett's test for post-hoc pair-wise comparisons.

Results

Exposure to blast overpressure alters cerebrovascular reactivity in a time-dependent manner

For each time point assessed post-BOP exposure, a total of 90–136 vessel measurements of pial arteriolar diameters were obtained. Previous work from our lab[30,37] and others[38] have demonstrated that vascular responses to local or systemic (intravenous) administration of vasoactive substances are different in small versus larger vessels within the microcirculation. The amount of smooth muscle as well as the presence of pericytes and other factors that affect vascular contractility vary considerably between small and larger vessels and capillaries lack smooth muscle altogether.[27] Therefore, we examined the relationship between vessel diameter/size and responsiveness to the vasoactive mediators evaluated in this study by grouping vessels into size categories, as previously described.[30,31,37] Responses of small (<50 μm) and medium (50–100 μm) sized vessels were compared across the different time points examined in this study. Overall, in sham animals, the three vasoactive mediators used in this study elicited responses that were consistent with the previously established normal vascular reactivity induced by these agents (Fig. 1); specifically, CO_2 resulted in ~4% vasodilation whereas $BaCl_2$ and 5-HT caused ~24% and 1% constriction, respectively.

Response to CO_2. Hypercapnia-induced dilation of cerebral blood vessels is a nitric oxide (NO)-dependent mechanism that significantly increases cerebral blood flow (CBF) to match tissue metabolic demands, and disruption of this phenomenon is an indication of impairment in vascular regulatory mechanisms. An example of pial arteriolar CO_2-induced dilation is illustrated (Fig. 2A,B). For each time point examined, 44–92 vessel measurements were analyzed in the small vessel category and 41–46 in the medium vessel category. The vascular response to CO_2 was different in small- compared to medium-sized vessels at 3 and 28 days (Mann-Whitney U test: $U = 17.37$ and 14.40 for 3 and 28 days, respectively; $p < 0.0001$ for each pair-wise comparison). Small vessels exhibited significant dilation compared to sham vessels at both 3 and 28 days (Fig. 2A; 3.74 ± 1.392% vs. 17.66 ± 3.077% for sham vs. 3 days post-blast, respectively; Mann-Whitney U: $U = 11.44$, $p < 0.01$; 3.74 ± 1.392% and 17.85 ± 2.873% for sham vs. 28 days post-blast, respectively; Mann-Whitney U: $U = 3.82$, $p < 0.01$).

On the other hand, medium vessels exhibited diminished dilation in response to CO_2 at all time points after blast compared to sham rats (Fig. 2B; Kruskal-Wallis: $\chi^2 = 19.58$, $p < 0.05$; Mann-Whitney U test: $U = 4.66$, 3.15, 5.12, 15.68, and 4.75 for sham vs. 2 h, 1, 3, 14, or 28 days, respectively; $p < 0.05$ for all pair-wise comparisons with sham). Unexpectedly, medium-sized vessels exhibited vasoconstriction 14 days post-BOP (−1.94 ± 1.061% compared to 4.071 ± 0.973% in sham rats; Mann-Whitney U test: $U = 15.68$, $p < 0.0001$). Thus, the data show a delayed disruption of hypercapnia-induced vasodilation with exposure to blast in both small- and medium-sized vessels. Most strikingly, CO_2-induced vasodilation was completely impaired in medium-sized arterioles.

Response to $BaCl_2$. Barium (barium ions in $BaCl_2$) is a relatively selective antagonist of inward rectifier potassium channels (K_{ir}) and adenosine triphosphate (ATP)-sensitive K^+ channels in vascular smooth muscle causing membrane depolarization of the cell and vasoconstriction.[39,40] Activation of both types of channels causes dilation of arteries and arterioles. $BaCl_2$ triggers vasoconstriction by inhibiting K^+ located on smooth muscle cells in the rat[41] through an endothelium-independent mechanism.[42] In both small- and medium-sized arterioles, treatment with $BaCl_2$ caused robust constriction of pial vessels in both sham and blast rats. However, pial arteriolar responses to treatment with $BaCl_2$ were distinct in small- compared to medium-sized vessels 2 h and 1 and 3 days post-BOP. Small-sized arterioles exhibited 3 times the constriction observed in medium-sized arterioles (Fig. 2C,D; 9.43 ± 3.209% to 13.24 ± 3.147% constriction in medium-sized vs. 30.22 ± 4.953% to 46.31 ± 4.358% in small-sized arterioles; Mann-Whitney U test: $U = 5.88$, 9.07, and 22.83 for 2 h and 1 and 3 days post-blast,

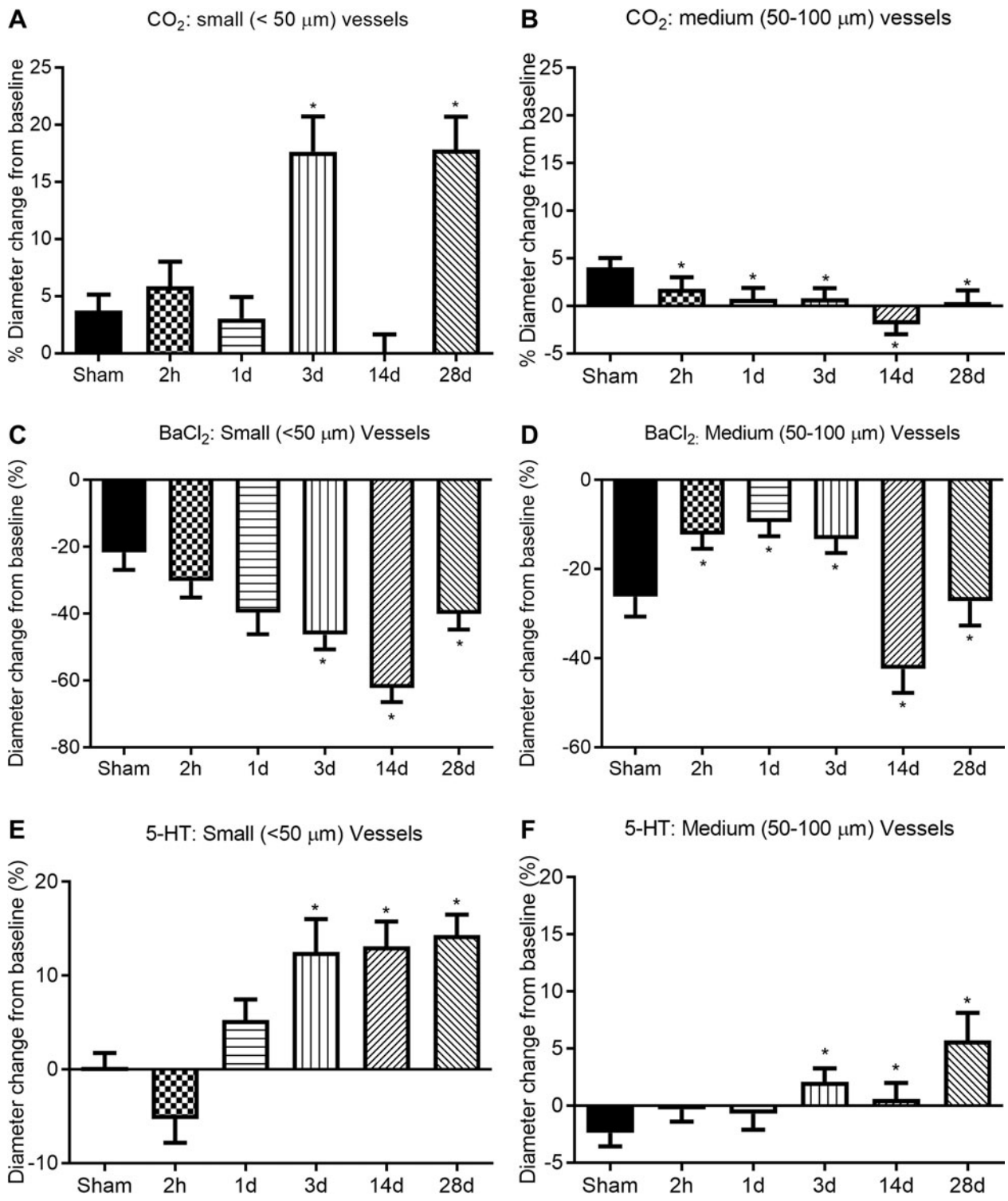

FIG 2. Intravital microscopy analysis of pial arteriolar vasoreactivity to hypercapnia (**A** and **B**), $BaCl_2$ (**C** and **D**), and 5-HT (**E** and **F**) in sham and blast-exposed rats. (A) Exposure to blast led to enhancement of the expected dilatory response in small-sized arterioles (<50 μm) 3 and 28d post-blast. (B) Medium-sized (50–100 μm) arterioles exhibited impaired vasodilation in response to CO_2 at all time points examined after exposure to blast. (C) Exposure to blast led to enhancement of barium-induced constriction in small-sized arterioles (<50 μm) 3–28d post-blast. (D) Medium-sized (50–100 μm) arterioles showed enhanced constriction only 14d post-blast. (E) 5-HT-induced constriction was reversed to dilation in small-sized arterioles >1d post-blast. (F) 5-HT-induced constriction was also reversed to dilation in medium-sized arterioles (50- 100 μm) 3–28d post-blast. Data are mean ± standard error of the mean percentage change of arteriolar diameter relative to pre-treatment baseline after treatment with each of the vasoactive mediators. *$p < 0.05$ versus sham. 5-HT, 5-hydroxytryptamine.

respectively; $p < 0.05$ for all comparisons). Vasoconstrictive response to $BaCl_2$ in both vessel size categories peaked 14 days post-BOP, reaching a constriction of $62.26 \pm 4.185\%$ in small-sized arterioles and $42.43 \pm 5.330\%$ in medium-sized arterioles.

For small-sized arterioles, there was a statistically significant enhancement in barium-induced vasoconstriction 3, 14, and 28 days post-BOP (Fig. 2C; Mann-Whitney U test for 3, 14, or 28 days vs. sham, respectively: U = 11.53, 23.78, and 6.11; $p < 0.05$ for all pair-wise comparisons). For medium-sized arterioles, there was only enhancement in barium-induced constriction 14 days post-BOP exposure (Fig. 2D; Mann-Whitney U test: U = 6.02, $p < 0.05$). At 2 h and 1 and 3 days after blast exposure, medium-sized vessels showed reduced constriction to barium compared to sham (Fig. 2D; Mann-Whitney U test: U = 6.82, 10.24, and 4.17 for 2 h and 1 and 3 days vs. sham, respectively; $p < 0.05$ for all pair-wise comparisons). Thus, both small- and medium-sized pial arterioles show a delayed increase in barium-induced constriction that occurs 14 days after exposure to blast. Small-sized arterioles show increased sensitivity to the vasoconstricting effects of barium compared to medium-sized vessels.

Response to serotonin. 5-HT has been shown to have both constricting and dilating effects on pial microvessels,[43–45] depending on several factors that include the health of the endothelium and the initial tone of the vessels under study. In our study, the vasoconstrictive response to 5-HT was observed in sham animals and 2 h after blast exposure in both small- and medium-sized pial arterioles (Fig. 2E,F); however, 3 days post-blast exposure, arterioles in both vessel size categories exhibited a dilatory response to 5-HT that increased significantly with time after exposure (Mann-Whitney U test for small-sized arterioles in sham vs. 3, 14, and 28 days post-blast, respectively; U = 6.37, 9.20, and 30.51, with $p < 0.05$ for all comparisons; Mann-Whitney U test for medium-sized arterioles in sham vs. 3, 14, and 28 days post-blast, respectively, U = 8.83, 4.69, and 6.35; $p < 0.05$ for all comparisons).

The magnitude of the response to 5-HT was significantly greater in small vessels (12.5 ± 3.52 to $14.31 \pm 2.18\%$) compared to medium-sized vessels (0.59 ± 1.40 to $5.69 \pm 2.44\%$) at 3, 14, and 28 days post-BOP (Fig. 2E,F; Mann-Whitney U test: U = 3.93, 7.66, and 8.78 for 3, 14, and 28 days post-blast, respectively; $p < 0.05$ for all comparisons). It is noteworthy that the responses to 5-HT of all the vessels examined were never biphasic; that is, a vessel either responded with constriction only or dilation in response to 5-HT application. The intravital microscopy data provide direct evidence that exposure to blast led to reversal of the vascular response to 5-HT from constriction to dilation.

Taken together, the intravital microscopy data demonstrate that exposure to blast leads to impairment in vascular reactivity that is not simply (or completely) attributed to direct mechanical deformation of the vessel as most of the changes occurred 24 h after blast and later. The data show that medium-sized vessel responses to the different vasoactive mediators were less pronounced than the responses of smaller arterioles. In addition, 14 days after exposure to blast, both small- and medium-sized pial arterioles exhibit enhanced contractility compared to other time points examined here, with diminished or absent dilation to CO_2 and the maximum amount of constriction observed in this study to $BaCl_2$. This phenomenon occurring 14 days post-blast was more pronounced in medium-sized vessels. The delayed loss of dilatory ability and increase in contractility may be an indication of an altered vascular phenotype that favors constriction, a process that involves remodeling of the vascular wall as previously suggested by *in vitro* work.[14] Additionally, the time course of the changes in vascular reactivity is consistent with clinical findings of the delayed onset of cerebral vasospasm in blast casualties.[3]

Alterations in vascular reactivity are not caused by differences in blood pressure, pH, or blood gases

It is well established that arterial blood pressure affects cerebrovascular tone and vessel size/diameter through autoregulatory mechanisms.[46–48] Also, other physiological variables, including body temperature, blood pH, and arterial blood gas tensions (p_aCO_2 and p_aO_2), may affect cerebrovascular tone. Therefore, during the intravital microscopy studies, mean arterial blood pressure (MAP), HR, body temperature, pH, p_aO_2, and p_aCO_2 were experimentally controlled and monitored. The collected data were compared among animals within the different experimental groups to rule out the effects of these variables on the observed responses of pial arterioles to the vasoactive mediators used in the study. MAP, HR, and body temperature values were collected every 5 min and compared before, during, and after stimulation with each of the three vasoactive mediators used in this study. Arterial blood samples were used for comparing pH, p_aO_2, and p_aCO_2 data. None of these variables were significantly different among the groups or between any pair at any point during the experiment. Table 1 summarizes the mean values (±SEM) of these physiological parameters of all the time points and animals within each experimental group.

Table 1. Blood Pressure, Vital Signs, and Blood Gas Parameters

	Sham	*2h*	*1d*	*3d*	*14d*	*28d*
MAP (mm Hg)	94 ± 4	88 ± 4	86 ± 3	87 ± 4	88 ± 3	90 ± 3
HR (beats/min)	399 ± 18	375 ± 22	439 ± 16	395 ± 18	402 ± 16	402 ± 13
Temp (^oC)	36.8 ± 0.1	36.8 ± 0.1	36.8 ± 0.1	36.8 ± 0.1	36.8 ± 0.1	36.7 ± 0.1
pH	7.268 ± 0.023	7.278 ± 0.031	7.268 ± 0.034	7.151 ± 0.292	7.288 ± 0.032	7.289 ± 0.027
p_aCO_2 (mm Hg)	52.7 ± 3.6	52.5 ± 5.1	56.2 ± 5.9	54.4 ± 5.2	52.9 ± 5.3	52.5 ± 4.8
p_aO_2 (mm Hg)	167.8 ± 7.3	176.0 ± 6.8	152.5 ± 10.6	172.2 ± 7.1	164.1 ± 4.9	165.9 ± 9.1

2h indicates 2 h post-blast exposure; 1, 3, 14, and 28d are 1, 3, 14, and 28 days post-blast exposure. $paCO_2$ and paO_2 represent arterial partial pressures of carbon dioxide and oxygen, respectively. No statistically significant differences in any of these parameters were found among any of the treatment groups, and therefore values are mean values ± standard error of the mean over the entire duration of the intravital microscopy studies for all animals studied.

MAP, mean arterial blood pressure; HR, heart rate.

Exposure to blast is associated with loss of vascular smooth muscle contractile proteins

To investigate the changes in cerebrovascular structure associated with alterations in cerebrovascular reactivity after blast exposure, we studied the contractile structural components of blood vessels. Based on findings from previous studies,[13,14] we hypothesized that changes in vascular smooth muscle cell structure may contribute to changes in vascular reactivity after exposure to blast. To that end, we examined and compared the expression of smooth muscle contractile proteins (SMTH, SM-MHC, SMA, and MLC) in sham- and blast-exposed rats. We first confirmed the localization of these proteins to the vessel wall in the rat cerebral vasculature using IHC to visualize colocalization of these proteins with smooth muscle (i.e., SMA; Fig. 3). Immunoreactivity of the four proteins was highly specific to the vasculature and SMTH, SM-MHC, and MLC colocalized with SMA (Fig. 3).

We examined whether blast exposure led to changes in thickness of vascular smooth muscle layers within the vessel wall. To address this question, we used IHC to label vascular smooth muscle in sham- and blast-exposed brain tissue sections with SMTH antisera. Immunoreactivity of SMTH (Fig. 3) was only observed in the vasculature, with high-fidelity colocalization with SMA, and almost no non-vascular or non-specific labeling. Therefore, SMTH served as a highly specific marker for vascular smooth muscle and was used for obtaining measurements of wall thickness of SMTH immunolabeled vessels (Fig. 4A,B). Wall thickness of each vessel was divided by lumen diameter to control for the effects of vessel size on smooth muscle thickness within the wall. Neither vessel thickness nor diameter was different among the sham- and blast-exposed groups examined (Fig. 4C; wall thickness was $5.41 \pm 0.10\,\mu$m [mean $\pm$ SEM; $n = 681$ vessels]).

We next used analysis of immunofluorescence intensity of immunolabeled brain sections (Fig. 5) and western blotting to determine changes in vascular smooth muscle contractile protein expression after exposure to blast. There was a decrease in SMTH immunoreactivity that started 1 day post-blast and reached statistical significance 3 and 28 days post-blast (Fig. 6A; ANOVA: $F_{(5,24)} = 2.70$, $p < 0.05$; Dunnett's: $p < 0.05$ for sham vs. 3 and 28 days post-blast and $p = 0.059$ for sham vs. 14 days post-blast). Similarly, expression of SMTH showed a significant reduction (30–50% compared to sham) when assayed by western blotting in blast-exposed rats 3–28 days after blast-TBI (Fig. 6B; ANOVA: $F_{(5,28)} = 3.68$, $p < 0.05$; Dunnett's: $p < 0.05$ for sham vs. 1, 3, 14, and 28 days post-blast). The vessel wall thickness data of SMTH-labeled vessels combined with the immunofluorescence and western blot findings demonstrate that the loss in this contractile protein was 1) pervasive, affecting vessels of different thickness and sizes (diameters) equally, and 2) that the delayed decrease in the expression of SMTH did not correlate with decrease in the thickness of the vascular smooth muscle layer.

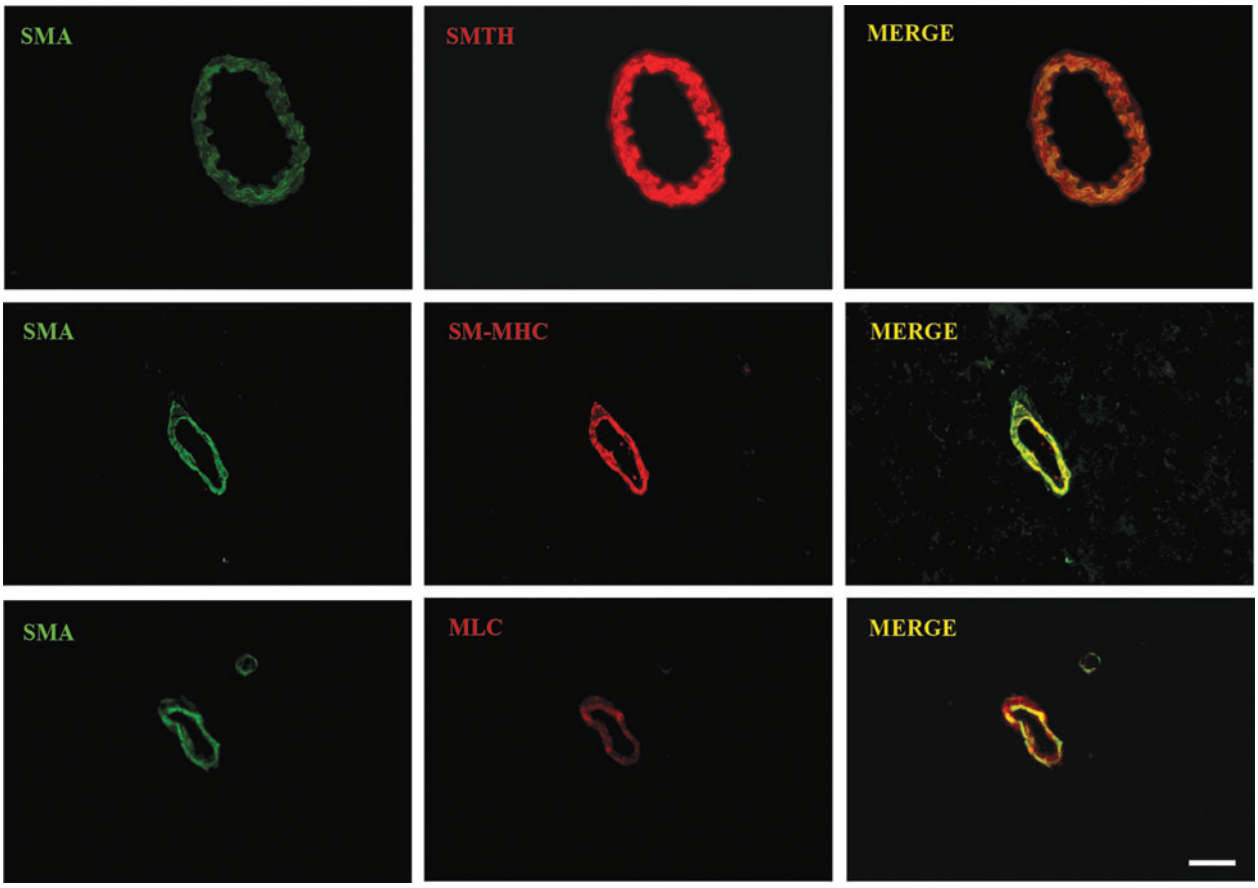

FIG 3. Colocalization of SMA, SMTH, SM-MHC, and MLC to the vasculature. SMA was used as a marker for contractile vascular smooth muscle and combined with antibodies against SMTH, SM-MHC, and MLC to confirm localization of these smooth muscle proteins to the vasculature in the cortex of Long Evans rats. Scale bar, 25 μm. MLC, myosin light chain; SMA, smooth muscle actin; SM-MHC, smooth muscle myosin heavy chain; SMTH, smoothelin.

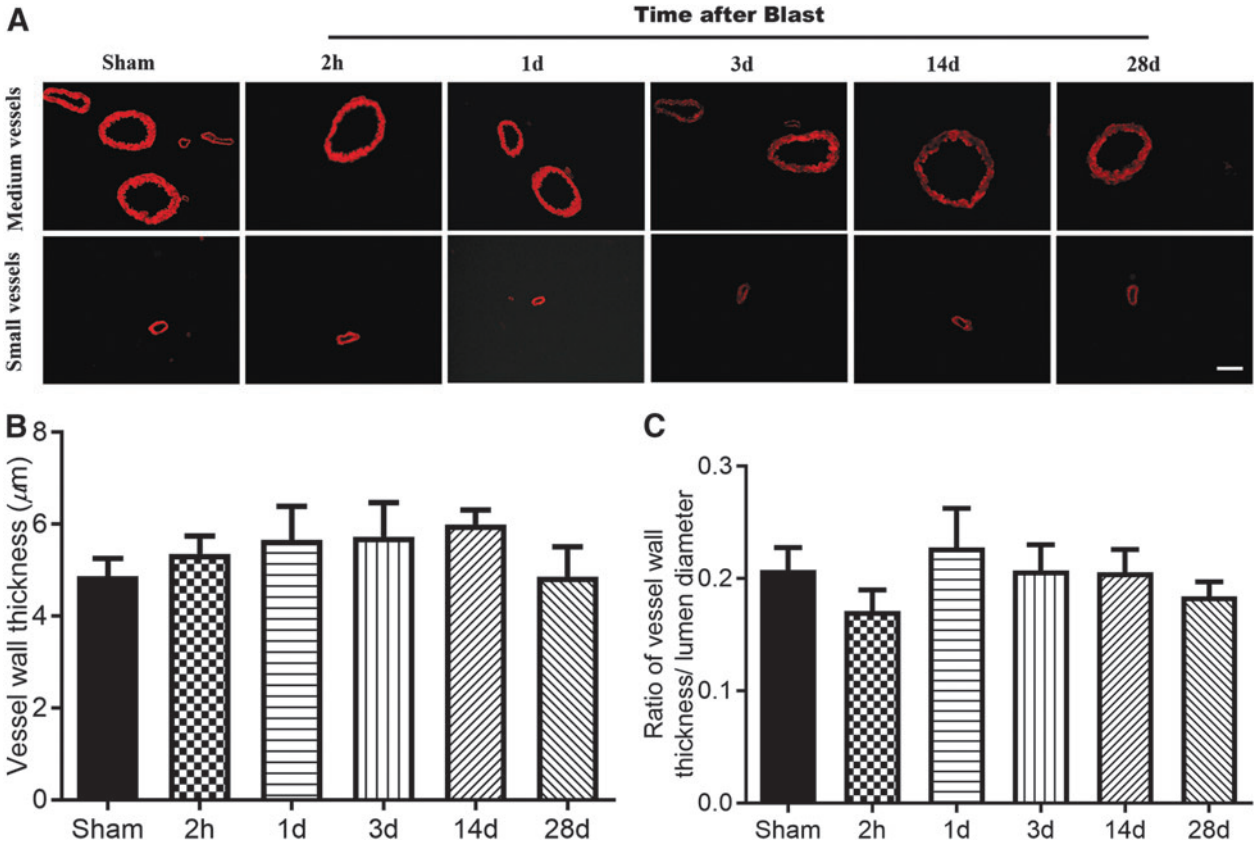

FIG 4. Exposure to blast does not alter microvessel wall thickness. (**A**) SMTH-immunolabeled small- and medium-sized microvessels in sham- and blast-exposed rats examined 2 h and 1, 3, 14, and 28 days after exposure to a single ~130-kPa blast. Scale bar, 25 μm. (**B**) Measurements of vessel wall thickness (mean ± standard error of the mean) did not change after blast exposure at any of the time points examined. (**C**) Vessel wall thickness was normalized to the lumen diameter of each measured vessel to correct for vessel diameter. Data are mean ± standard error of the mean. SMTH, smoothelin.

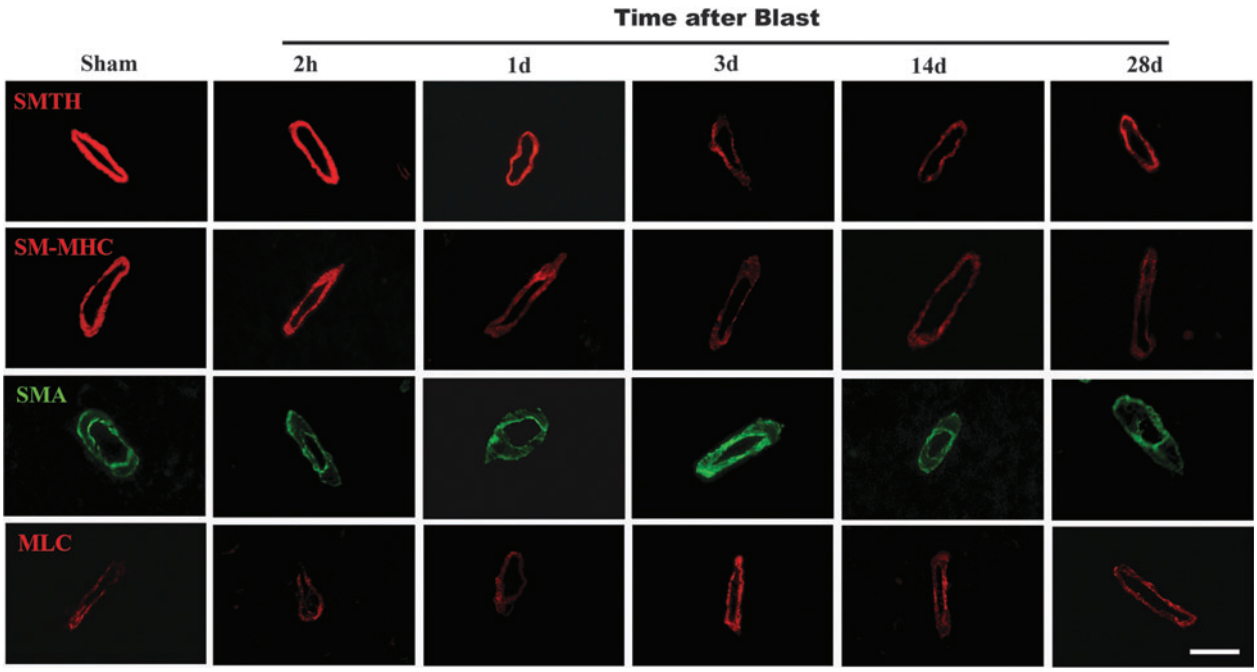

FIG 5. Expression of smooth muscle proteins after exposure to blast. Brain sections from sham- and blast-exposed rats were probed with antibodies against SMTH, SM-MHC (MYH11), SMA (α-actin), and MLC to study the time course of changes in immunofluorescence intensity in cortical microvessels 2 h and 1, 3, 14, and 28 days after blast exposure. Scale bar, 25 μm. MLC, myosin light chain; SMA, smooth muscle actin; SM-MHC, smooth muscle myosin heavy chain; SMTH, smoothelin.

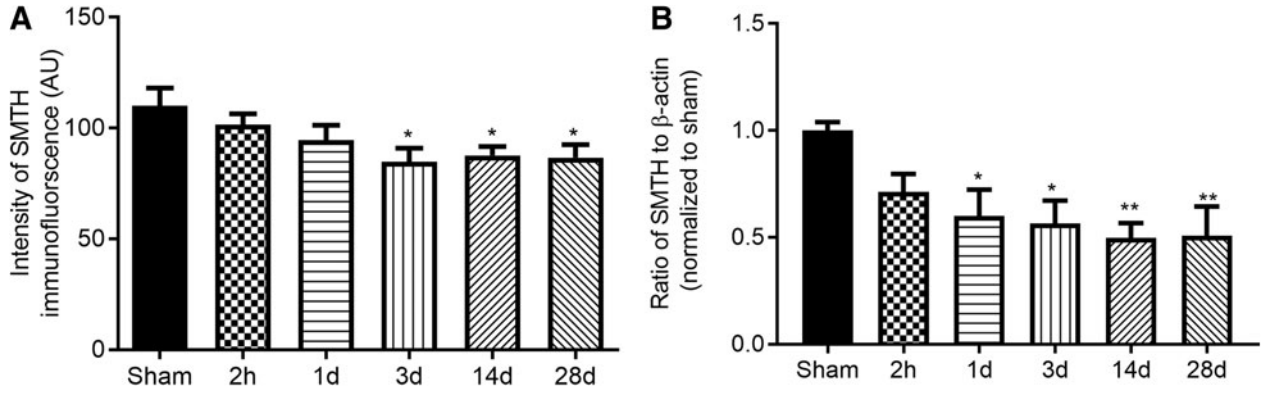

FIG 6. Delayed reduction in the expression of SMTH after blast exposure. (**A**) Immunofluorescence intensity (arbitrary units; AU) assessment of SMTH-immunolabeled microvessels in sham- and blast-exposed rats ($n=5$ rats/group). SMTH immunofluorescence intensity (mean ± standard error of the mean) decreased 3–28 days post-blast. *$p<0.05$ versus sham. (**B**) Semiquantitative analysis of western blots of frontoparietal cortex (mean ± standard error of the mean normalized to sham values) shows a reduction in SMTH expression 1–28 days post-blast exposure ($n=6$ rats/group). *$p<0.05$; **$p<0.01$ versus sham. SMTH, smoothelin.

Similar to the SMTH data, SM-MHC expression decreased by ~55–80% of the sham values 1, 3, 14, and 28 days post-blast in immunofluorescence (Fig. 7A; ANOVA: $F_{(5,24)}=5.56$, $p<0.01$; Dunnett's: $p<0.05$ for sham vs. 1, 3, 14, and 28 days post-blast) and western blot studies (Fig. 7B; ANOVA: $F_{(5,28)}=14.58$, $p<0.0001$; Dunnett's multiple comparisons: $p<0.005$ for sham vs. 1, 3, 14, or 28 days post-blast). Immunofluorescence intensity analysis of SMA showed a different pattern from SMTH and SM-MHC; specifically, immunofluorescence intensity of SMA increased 3 days post-blast (Fig. 8A; ANOVA: $F_{(5,24)}=1.80$, $p=0.15$, i.e., statistically not significant; Dunnett's: $p<0.05$ for sham vs. 3 days post-blast). Western blot data, on the other hand, showed that SMA expression decreased 28 days post-blast to 44% of the sham value (Fig. 8B; ANOVA: $F_{(5,30)}=2.60$, $p<0.05$; Dunnett's: $p<0.05$ for sham vs. 28 days post-blast). The cause of the discrepancy between immunofluorescence intensity and western blot analysis is unknown. A possible explanation is that assessment of immunofluorescence intensity is based on the subset of vessels present within the field of view of the microscope and selected for assessment, whereas western blotting yields a whole sample (brain region in this study) signal and is therefore the more sensitive, global, and less biased assay.

The phosphorylation state of MLC regulates the actin-myosin interactions in vascular smooth muscle cells. In the cerebral vasculature, MLC is found in both endothelial and smooth muscle cells. Although the signaling mechanism remains unknown, enhancement in the phosphorylation of MLC is associated with certain vascular pathologies, including TBI[49] and enhancement in vasoconstriction in cerebral vasospasm.[50,51] Here, we found that exposure to blast leads to a delayed sustained increase in immunofluorescence intensity of total MLC, with ~36–88% increase relative to sham values 1–28 days after blast exposure (Fig. 9A; ANOVA: $F_{(5,24)}=4.06$, $p<0.01$; Dunnett's: $p<0.01$ for sham vs. 3 and 28 days post-blast). Similarly, western blot analyses showed an increase in total MLC beginning 3 days post-blast and persisting up to 28 days post-blast, where the levels of MLC were 41% higher than sham (Fig. 9B; ANOVA: $F_{(5,30)}=5.52$, $p<0.01$; Dunnett's: $p<0.01$ for sham vs. 28 days post-blast). Changes in phosphorylation of MLC were also delayed, and, although not statistically significant, there was an 18% increase in phosphorylation of MLC

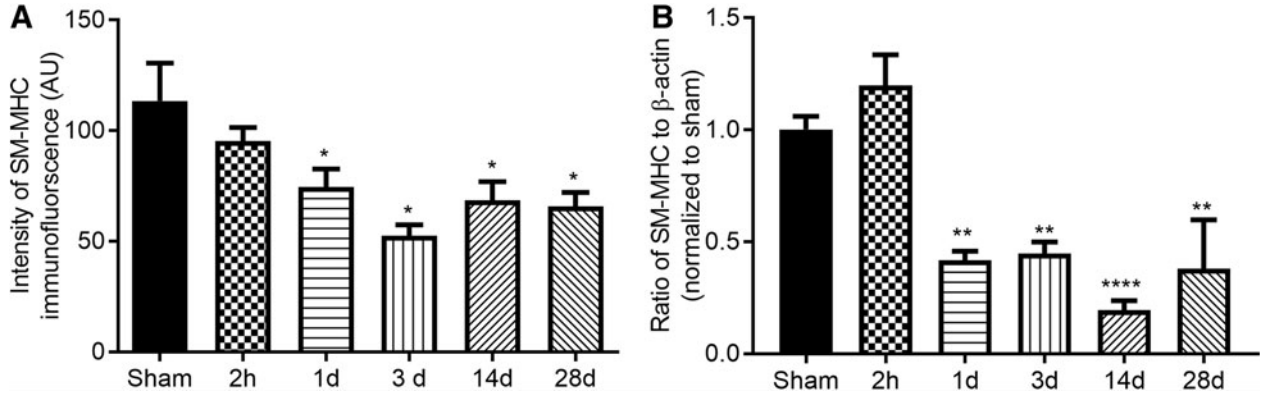

FIG 7. Blast-induced delayed reduction in the expression of SM-MHC mirroring reduction in SMTH expression. (**A**) Immunofluorescence intensity (arbitrary units; AU) assessment of SM-MHC–immunolabeled microvessels in sham- and blast-exposed rats ($n=5$ rats/group). SM-MHC immunofluorescence intensity (mean ± standard error of the mean) decreased 3–28 days post-blast. *$p<0.05$ versus sham. (**B**) Semiquantitative analysis of western blots of frontoparietal cortex (mean ± standard error of the mean normalized to sham values) show a reduction in SM-MHC expression 1–28 days post-blast exposure ($n=6$ rats/group). **$p<0.01$; ****$p<0.000$ versus sham. SM-MHC, smooth muscle myosin heavy chain; SMTH, smoothelin.

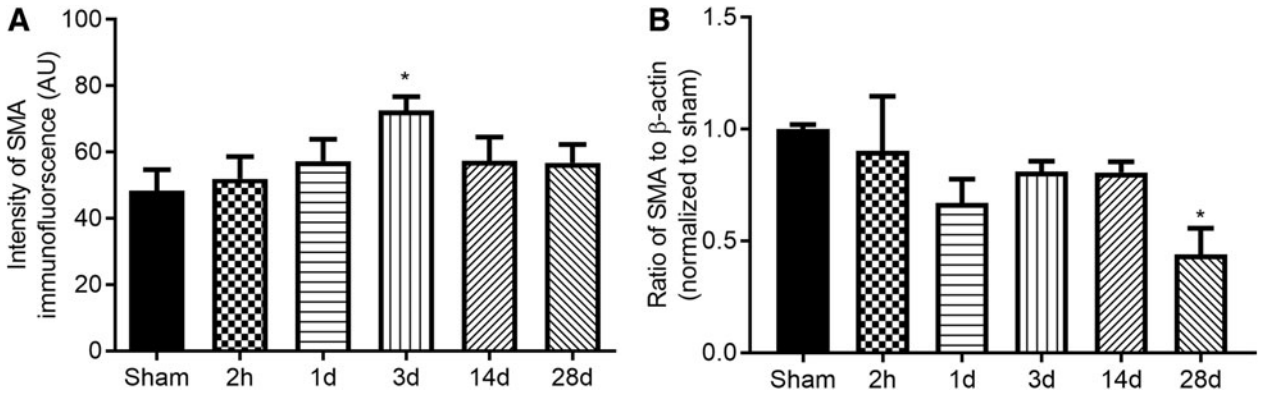

FIG 8. Delayed reduction in the expression of SMA after exposure to blast. (**A**) Immunofluorescence intensity (arbitrary units; AU) assessment of SMA-immunolabeled microvessels in sham- and blast-exposed rats ($n=5$ rats/group). SMA immunofluorescence intensity (mean ± standard error of the mean) increased 3 days post-blast. *$p<0.05$ versus sham. (**B**) Semiquantitative analysis of western blot of frontoparietal cortex (mean ± standard error of the mean normalized to sham values) shows a ~50% reduction in SMA expression 28 days post-blast exposure ($n=6$ rats/group). *$p<0.05$ versus sham. SMA, smooth muscle actin.

on day 14 post-blast (Fig. 9C). At 28 days post-blast, levels of p-MLC showed a 75% reduction compared to non-blast sham brains (Fig. 9D; ANOVA: $F_{(5,29)}=3.89$, $p<0.01$; Dunnett's: $p<0.01$ for sham vs. 28 days post-blast).

Analyzing the ratio of p-MLC to total MLC is a helpful approach to understanding how an increase or decrease in phosphorylation levels of a protein relates to expression of the protein after exposure to blast. Predictably, the ratio was lowest 28 days post-blast because expression of MLC was highest and that of p-MLC was lowest 28 days post-blast (Fig. 9D; ANOVA: $F_{(5,30)}=7.06$, $p<0.001$). Based on analysis of phosphorylated-to-total MLC, it can be concluded that the decrease in phosphorylation of MLC is not caused by a decrease in the expression of MLC 28 days post-blast. Representative immunoblots of total and phosphorylated MLC are shown in Figure 9.

Overall, analyses of smooth muscle proteins show that exposure to blast leads to delayed reduction in markers of contractile vascular smooth muscle cells (SMTH, SM-MHC, and SMA) and increase in MLC. These changes signal a shift in the phenotype of vascular smooth toward a non-contractile phenotype and indicate changes in smooth muscle contractility, most markedly suggested by changes in MLC.

Endothelial-related changes after blast exposure

In addition to effects on vascular smooth muscle, alterations in cerebral vascular reactivity after exposure to blast can result from impairment in the vascular endothelium. The endothelium regulates vessel tone by producing vasoactive substances, including ET-1 and NO, which control the myogenic state of vascular smooth muscle. To understand blast-induced changes within or directly affecting the endothelium, we assessed expression of NO-producing eNOS and iNOS, ET-1, and the two ET-1 receptor types (ET_A and ET_B).

Although eNOS and iNOS serve different functions, there was a delayed decrease in the levels of both enzymes after blast exposure. The levels of eNOS decreased 1–14 days post-blast and reached a 62% reduction compared to sham levels 14 days post-blast (Fig. 10A; ANOVA: $F_{(5,29)}=7.44$; Dunnett's for sham vs. 14 days post-blast; $p<0.05$), followed by a non-significant increase 28 days after blast. Although previous reports showed that blast exposure is associated with increase in iNOS in the acute phase,[52] our study shows that iNOS levels decreased by ~55–60% 14 and 28 days after blast exposure (Fig. 10B; ANOVA: $F_{(5,29)}=3.75$, $p<0.01$; Dunnett's: $p<0.05$ for sham vs. 14 days and sham vs. 28 days). These data suggest that exposure to blast is associated with a delayed decrease in NO availability that lasts up to a month after blast exposure.

We next examined the endothelin system because it is highly implicated in the pathogenesis of cerebral vasospasm. ET-1 is produced and released by endothelial cells lining the vasculature. There was an increase in both ET-1 and the biologically inactive ''big'' ET-1 levels relative to sham in frontoparietal cortical tissue within 2 h after exposure to blast (Fig. 11A–C; ANOVA: for ET-1 $F_{(5,30)}=3.01$, $p<0.05$ and Dunnett's: $p<0.05$ for sham vs. 2 h post-blast; for big ET-1 $F_{(5,30)}=3.85$ $p<0.01$ and Dunnett's: $p<0.05$ for sham vs. 2 h post-blast) that returned to sham levels at later time points examined. As such, blast exposure results in a significant (2-fold relative to non-blast shams) increase in biologically active ET-1 levels in the acute phase after exposure. To further understand blast-induced changes in ET-1, we examined expression of ET_A and ET_B receptors and sought to answer the following two questions. 1) How does blast exposure affect the overall expression of ET_A and ET_B? 2) Does exposure to blast induce redistribution of either receptor from microvessels to astrocytes or vice versa?

To address the first question, we examined the effects of blast exposure and time on ET_A and ET_B. Immunofluorescence intensity analysis of ET_A immunoreactivity showed an increase in ET_A expression in the early phases after blast exposure, specifically, 1 and 3 days post-blast relative to sham (Fig. 11D; ANOVA: $F_{(5,24)}=5.13$, $p<0.01$; Dunnett's: $p<0.05$ for sham vs. 1 and 3 days). Western blot data, which present a more global picture of changes in ET_A, revealed a 28% decrease in the receptor expression 14 days post-blast and 33% increase 28 days post-blast (Fig. 11E,F; ANOVA: $F_{(5,29)}=9.89$, $p<0.0001$; Dunnett's: $p<0.05$ for sham vs. both 14 and 28 days). The difference between the IHC and blotting data may be attributed to differences in the assays utilized: Immunofluorescence analyses are based on several sections per rat, whereas protein blots are based on frontoparietal cortex tissue homogenate.

Analysis of immunofluorescence of the ET_B receptor revealed a gradual increase in the expression of the receptor with time after

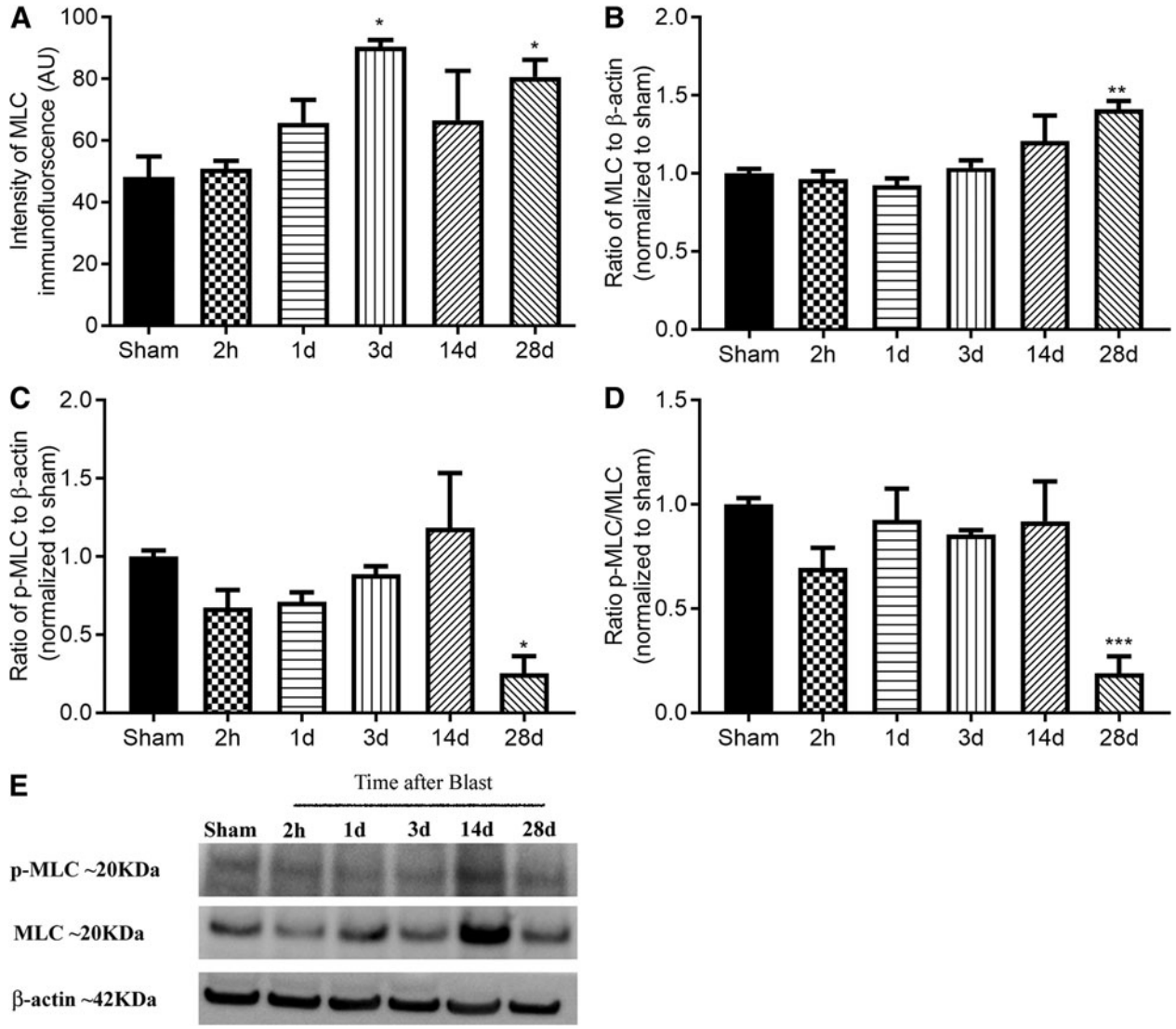

FIG 9. Delayed increase in the expression of smooth muscle MLC after blast exposure. (**A**) Immunofluorescence intensity (arbitrary units; AU) assessment of MLC-immunolabeled microvessels in sham- and blast-exposed rats ($n=5$ rats/group). MLC immunofluorescence intensity (mean ± standard error of the mean) increased beginning 3 days post-blast and remained elevated until 28 days after exposure. *$p<0.05$ versus sham. (**B–D**) Western blot density analysis (mean ± standard error of the mean) of total (**B**), phosphorylated (**C**), and ratio of phosphorylated-to-total MLC (**D**) in frontoparietal cortex in sham- and blast-exposed rats. (**B**) Semiquantitative analysis of blot density show a ~50% in MLC expression 28 days post-blast exposure. **$p<0.01$ versus sham. (**C**) Phosphorylation of MLC at Ser19 showed a statistically non-significant increase ~20% increase 14 days post-blast, which then decreased by ~75% 28 days after exposure. *$p<0.05$versus sham. (**D**) The ratio of phosphorylated-to-total MLC show that the decrease in MLC phosphorylation 28 days post-blast was not attributed to a reduction in the total levels of MLC. ***$p<0.001$ versus sham. (**E**) Immunoblots of MLC and phospho-MLC tissue lysates. Each band is a single representative animal from each group studied ($n=6$ rats/group). MLC, myosin light chain; p-MLC, phosphorylated myosin light chain.

blast exposure that peaked 28 days post-blast (Fig. 11G; ANOVA: $F_{(5,24)}=2.44$, $p=0.06$; Dunnett's: for sham vs. 28 days, $p<0.05$). Levels of ET_B in western blot also exhibited a gradual increase with time after blast exposure that doubled ET_B 14 days after injury (Fig. 11H,I; ANOVA: $F=17.02$, $p<0.0001$; Dunnett's: $p<0.0001$ for sham vs. 14 days). In the case of ET_B, the data from both assays clearly demonstrate a pattern of delayed increase in the expression of this receptor.

To address the question of whether exposure to blast leads to changes in the distribution of ET_A and/or ET_B within the vascular or astrocytic compartments, we examined the colocalization of the endothelin receptors with SMA (used as a marker of microvessels) and GFAP (used a marker of astrocytes). Under normal conditions, ET_A expression in the rat cortex predominantly colocalized with smooth muscle and not with astrocytes (Fig. 12A). However, some very low levels of ET_A immunoreactivity was observed on non-vascular and non-astrocytic cells, presumably neurons, as previously described in rat brain.[53] Unlike the ET_A receptor, ET_B receptor colocalized to both vascular smooth muscle and astrocytes (Fig. 12B). Exposure to blast did not correlate with changes in colocalization of ET_A with microvessels or astrocytes (data not shown).

In contrast, ET_B colocalization with astrocytes increased gradually 3–28 days after blast exposure (Fig. 12C; arrows), reaching a

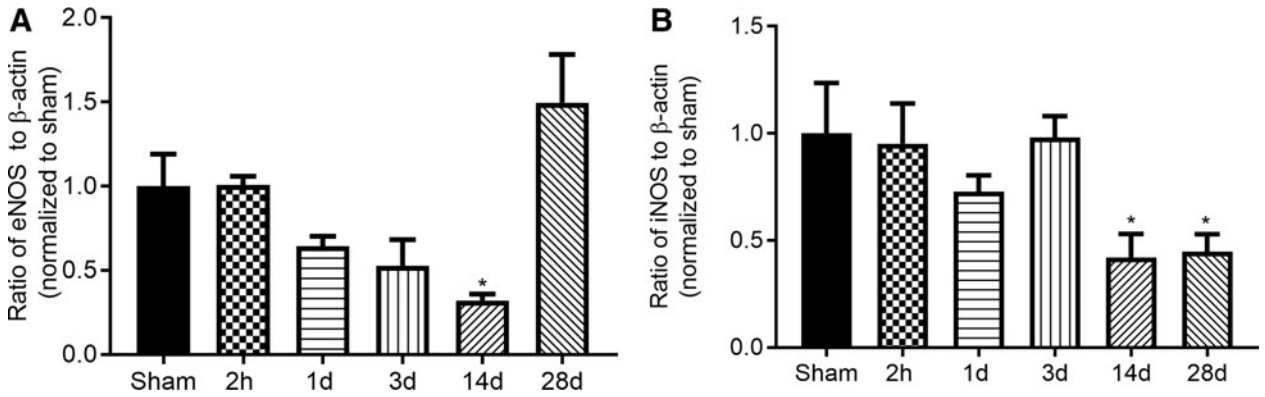

FIG 10. Decline of expression of nitric oxide synthase (NOS) after blast exposure as measured by western blot analysis. (**A**) Endothelial NOS (eNOS) levels decreased gradually after blast exposure reaching a >50% reduction 14 days post-blast. (**B**) Blast exposure resulted in a delayed reduction in inducible NOS (iNOS) 14 and 28 days post-blast. In (**A**) and (**B**), data are mean band density ± standard error of the mean ($n = 6$ rats /group); $^*p < 0.05$ versus sham.

~30% increase relative to sham by 28 days post-blast (Fig. 12D; ANOVA: $F_{(5,24)} = 2.97$, $p < 0.05$; Dunnett's $p < 0.01$ for sham vs. 28 days). In the meantime, the density of ET_B on SMA-positive vascular elements remained unchanged. The increase in astrocytic ET_B after blast exposure cannot be simply attributed to astrogliosis. GFAP expression was examined and a 15–20% *reduction* was observed in IHC (Fig. 12E) and western blot (Fig. 12F; ANOVA: $F_{(5,29)} = 5.95$, $p < 0.05$; Dunnett's: $p < 0.05$ for sham vs. 2 h) within the first 2 h post-blast. Levels of GFAP were unchanged at the later time points post-blast when ET_B levels were on the rise.

Collectively, these data show that exposure to blast increases ET-1 production in the acute phase, whereas impairment in NO production and changes in ET-1 receptors occur in the later phase (>24 h). In particular, the data demonstrate exposure to blast is associated with a delayed increase in the expression of ET_B and concomitant redistribution of the receptor from the vessel wall to astrocytes. Our observations establish that the effect of blast exposure on astrocytes is more complex than reactive astrogliosis and involves a delayed change in the phenotype of astrocytes as evidenced by the increase in the expression of ET_B on these cells.

Discussion

Impaired vascular reactivity is a major contributor to various neuropathological conditions including TBI[54,55] and cerebral vasospasm.[16] The effects of exposure to blast overpressure on cerebral microvascular reactivity are largely unknown as are blast-induced pathological changes in the vasculature initiating post-blast vasospasm. The principle finding of the present study is that exposure to blast leads to prolonged impairment in vasoreactivity of the pial microcirculation and changes in the structure and phenotype of cerebral vessels and astrocytes. We provide direct evidence *in vivo* that cerebral arterioles exhibit diminished vasodilation and enhanced constriction >24 h after blast exposure, with a peak 14 days post-blast. The role of serotonin was reversed from constrictor to dilator of pial arterioles up to 28 days after exposure to blast. Within the same time frame, cortical microvessels underwent changes in vascular smooth muscle contractile proteins, endothelial proteins, and endothelin receptor density in astrocytes. The changes in vascular architecture may contribute to alterations of cerebrovascular tone and the observed change in cerebrovascular reactivity. Our findings indicate that exposure to blast induces remodeling not only in the vasculature, but also in the astrocytic compartment of the neurovascular unit.

Exposure to blast overpressure impairs microvascular vasodilation

The vasodilatory effects of hypercapnia, including in pial arterioles, are widely believed to be mediated by production of NO.[56–58]

FIG 11. Alterations in the levels of endothelin-1 (ET-1) and the endothelin receptors, ET_A and ET_B, after blast exposure. (**A–C**) Western blot analysis (mean ± standard error of the mean) of the levels of ET-1 and its biologically inactive precursor big ET-1. (**A**) Semiquantitative analysis of blot density showed a near 2-fold increase in the expression of ET-1 acutely (2 h) post-blast exposure. $^*p < 0.05$ versus sham. (**B**) Big ET-1 expression also shows a significant increase 2 h after exposure. $^*p < 0.05$ versus sham. (**C**) Immunoblots of ET-1 and big ET-1 in cortical tissue lysate. Blots from representative animals are shown for each time point studied ($n = 6$ rats/group). (**D–F**) Expression of ET_A after blast exposure. (**D**) Immunofluorescence intensity (arbitrary units) assessment of ET_A immunoreactivity in microvessels in brain tissue sections. ET_A expression increased 1 and 3 days after blast. $^*p < 0.05$ versus sham. (**E**) Semiquantitative analysis of western blots (mean ± standard error of the mean) showed delayed changes in receptor expression 14 and 28 days post-blast exposure. A decrease in ET_A levels 14 days post-blast was followed by a 33% increase 28 days after exposure. $^*p < 0.05$ versus sham. (**F**) Immunoblots of ET_A in frontoparietal cortical tissue lysate. Blots from representative animals are shown for each time point studied ($n = 6$ rats/group). (**G–I**) Expression of ET_B after blast exposure. (**G**) Semiquantitative analysis of western blots showed a gradual delayed increase in ET_B expression, peaking 14 days post-blast exposure. $^*p < 0.05$ versus sham. (**H**) Immunofluorescence intensity (arbitrary units) assessment of ET_B immunoreactivity in microvessels in brain tissue sections. ET_B expression increased gradually >1 day post-blast, reaching a statistically significant increase (~30% relative to sham) by 28 days post-blast. $^{***}p < 0.001$ versus sham. (**I**) Immunoblots of ET_B in frontoparietal cortical tissue lysate. Bands in immunoblots are from 2 representative rats from each group studied ($n = 6$ rats/group). Error bars indicate standard error of the mean.

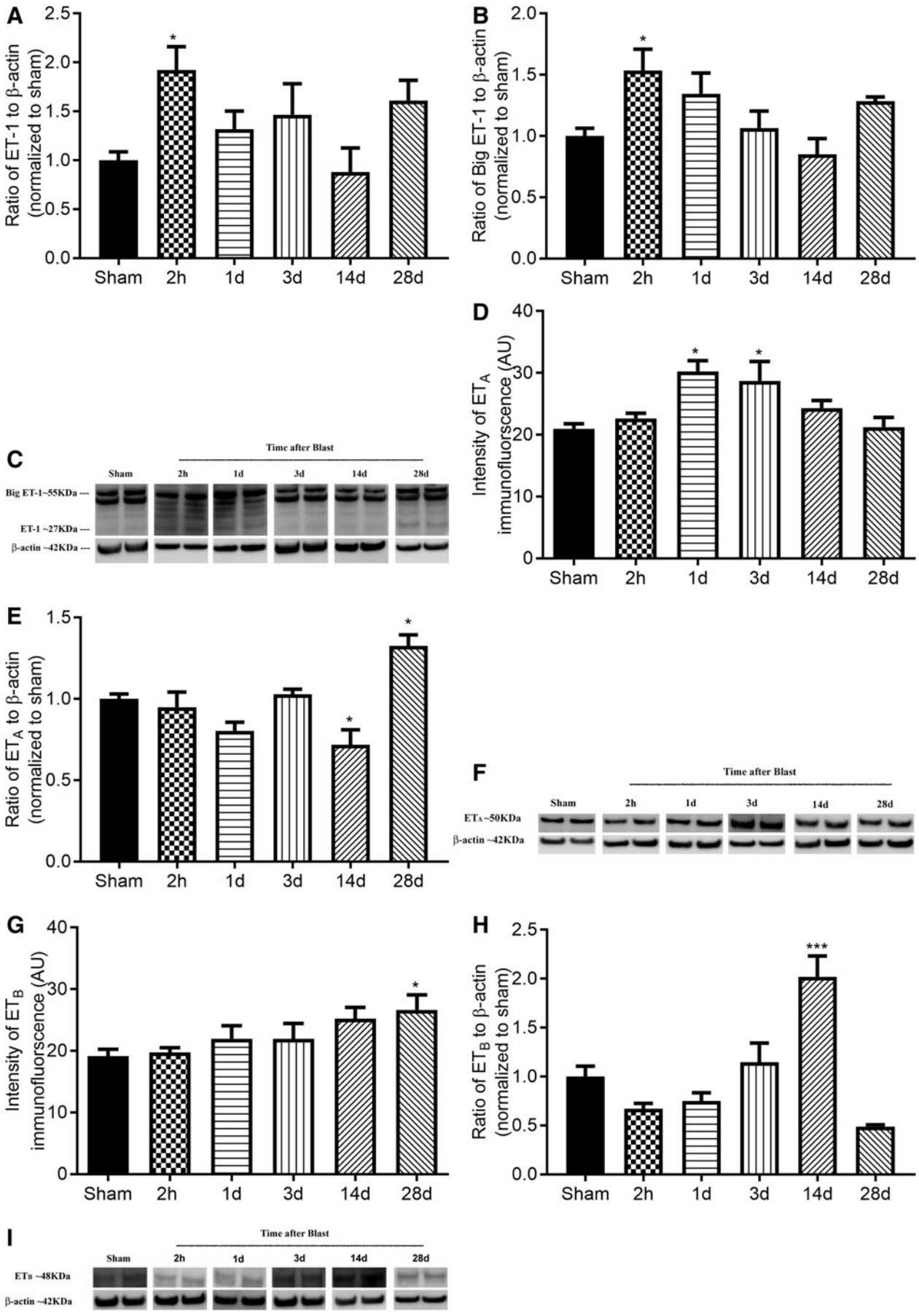
A
Ratio of ET-1 to β-actin (normalized to sham)
2.5
2.0
1.5
1.0
0.5
0.0
*
Sham
2h
1d
3d
14d
28d
B
Ratio of Big ET-1 to β-actin (normalized to sham)
2.0
1.5
1.0
0.5
0.0
*
Sham
2h
1d
3d
14d
28d
C
Time after Blast
Sham
2h
1d
3d
14d
28d
Big ET-1~55KDa ---
ET-1 ~27KDa ---
β-actin ~42KDa ---
D
Intensity of ETA immunofluorscence (AU)
40
30
20
10
0
*
*
Sham
2h
1d
3d
14d
28d
E
Ratio of ETA to β-actin (normalized to sham)
1.5
1.0
0.5
0.0
*
*
Sham
2h
1d
3d
14d
28d
F
Time after Blast
Sham
2h
1d
3d
14d
28d
ETA~50KDa
β-actin ~42KDa
G
Intensity of ETB immunofluorscence (AU)
40
30
20
10
0
*
Sham
2h
1d
3d
14d
28d
H
Ratio of ETB to β-actin (normalized to sham)
2.5
2.0
1.5
1.0
0.5
0.0
***
Sham
2h
1d
3d
14d
28d
I
Time after Blast
Sham
2h
1d
3d
14d
28d
ETB ~48KDa
β-actin ~42KDa

Vasodilation-induced CBF alterations in response to hypercapnia are impaired or abolished acutely after non-blast TBI, but recovery is observed within 2–10 days.[59] In our model, hypercapnia-induced vasodilation was abolished in arterioles (50–100 μm), both acutely and up to 28 days after blast exposure. Impaired CO_2 vasodilation is associated with endothelial dysfunction,[60] and increasing NO availability restores CO_2 reactivity after TBI.[61,62] Therefore, the observed increase in ET-1 acutely after blast exposure, delayed reduction in NOS, and increase in expression of ET_B receptors in this study may be associated with reduction in NO-mediated dilation and the observed altered response to CO_2. Blast-induced impairment in cerebral arterial dilation *ex vivo* was previously reported.[8,13] Our data extend this emerging view and demonstrate similar findings *in vivo*.

Regulation of the cerebral circulation by altering vessel diameter can vary with vessel size. In particular, the magnitude of the vasodilatory effects of CO_2 on pial arterioles depends on the resting vessel baseline diameter, with smaller arterioles exhibiting greater dilation than larger arterioles.[63,64] Dilation of larger arterioles has been shown to be more dependent on NO than that of smaller arterioles.[65,66] Our observations in sham animals did not show a difference in magnitude of dilation in the smaller (<50 μm) versus larger (50–100 μm) microvessels. However, the loss of hypercapnia-induced dilation after exposure to blast in the larger arterioles (50–100 μm) at all time points examined is consistent with a dysregulation of NO-mediated dilation mechanism explanation given that these vessels may be more sensitive to NO.

It is noteworthy that there is some controversy surrounding the role of NO in hypercapnia-induced cerebrovascular changes. Some reports failed to show an effect of NO synthase inhibition on CO_2-induced vasodilation in the cerebral vasculature,[67] whereas others demonstrated a combined effect of NO and potassium channels (e.g., ATP-sensitive channels).[68,69] Our studies were not designed to distinguish the different factors eliciting CO_2-induced vasodilation, and therefore the involvement of other mechanisms in the altered response to hypercapnia after exposure to blast cannot be ruled out.

Enhanced vasoconstriction may result from increase in endothelial vasoconstrictors[70] or decrease of vasodilators[43]; however, it can also result from changes in vascular smooth muscle. Smooth muscle barium-sensitive K_{ir} channels participate in CBF regulation by triggering vasodilation in response to extracellular K^+ generated by neuronal activity. The hyperpolarizing effects of K^+ associated with vasodilation are only found in contractile, and not proliferative, smooth muscle cells.[71] An increase in proliferative smooth muscle cells within the vessel wall would diminish the K_{ir}-mediated vasodilatory capacity of the vessel. Such a change would shift the balance of constricting and dilating factors acting on the vessel in favor of constriction. This is supported in this study by the significant reduction in smooth muscle contractile proteins after blast exposure (a change associated with shifting of smooth muscle cells to a proliferative phenotype) and increase in barium-induced constriction.

In the present study, the increase in barium-induced constriction after exposure to blast was observed as early 3 days post-blast in smaller arterioles (<50 μm), but appeared later (at 14 days) in the 50- to 100-μm vessel category. These differences in the time-course response of the microvasculature may be related to early versus delayed manifestations of blast-induced injurious processes. Whether differences in the amount of smooth muscle within the vessel wall contribute to these temporal dynamics changes in reactivity in smaller versus larger pial arterioles remains to be determined. The exact mechanism of the enhanced barium-induced vasoconstriction in vessels with fewer contractile smooth muscle cells after blast exposure remains unclear and warrants further investigation. The prolonged increase in barium-induced vasoconstriction and impaired CO_2 dilation (especially in the 50- to 100-μm vessels) reported here is consistent with reports of cerebral hypoperfusion after exposure to blast in rats that lasts up to at least 3 days.[72]

Whereas some investigations demonstrated that non-blast brain injury alters the expected cerebrovascular response to certain factors (e.g., neuronal activation or acetylcholine) from vasodilation to -constriction,[73,74] our study demonstrates that exposure to blast elicits an unexpected change in the microvascular response to serotonin from constriction to dilation. The finding that exposure to blast leads to reversal of the serotonin vasomotor effect from a constrictor to a dilator of pial arterioles may be related to several changes within the microvascular milieu. First, the phenomenon may be explained, in part, by differences in the initial tone of the vessels under study. Although most studies reported vasoconstriction of the pial vasculature in response to serotonin,[75,76] some studies reported a tone-dependent effect.[45,77,78] Specifically, Harper and MacKenzie[77] demonstrated that small pial arterioles (<70 μm in their study), which have the highest tone within the pial microcirculation, respond with dilation to locally applied serotonin whereas larger vessels respond with constriction.

In the present study and in agreement with the findings of Harper and MacKenzie, small pial arterioles (<50 μm in our study) showed a greater degree of dilation to serotonin than medium-sized vessels. In addition, reversal of serotonin-induced constriction has been reported after increasing vessel tone by chemical pre-constriction of pial arterioles before serotonin application.[45] Thus, the serotonin-induced vasodilation in our studies 1–28 days post-blast

FIG 12. Alteration in the distribution of ET_B receptors within the neurovascular unit after blast exposure. Colocalization of ET_A (**A**) and ET_B (**B**) receptors to vascular smooth muscle (SMA-positive) or astrocytes (GFAP-positive) under normal, sham conditions. (**A**) ET_A expression in the rat cortex predominantly colocalized with vascular smooth muscle and not with astrocytes. Scale bar, 25 μm. (**B**) ET_B receptor colocalized to both vascular smooth muscle and astrocytes. Scale bar, 25 μm. (**C**) Confocal micrographs of sham- and blast-exposed brain sections examined 28 days after blast exposure. ET_B colocalization with astrocytes (arrows) increased gradually after blast exposure, reaching a $\sim$30% increase relative to sham by 28 days post-blast. Scale bar, 50 μm. (**D**) Analysis of percentage of ET_B immunoreactivity colocalizing with GFAP-positive astrocytes showed an increase in percent of astrocytic ET_B 28 days after exposure. Data are mean $\pm$ standard error of the mean. $^{**}p < 0.05$ versus sham. Semiquantitative analysis of GFAP expression by analyzing (**E**) immunofluorescence intensity or (**F**) western blots after blast exposure showed that increase in astrocytic ET_B was not attributed to increase in GFAP (i.e., astrogliosis). Analysis of immunoblots in (**F**) showed that the only difference in GFAP levels occurred 2 h post-blast, where a decrease in GFAP levels were observed. Data in (**E**) and (**F**) are mean $\pm$ standard error of the mean. $^{*}p < 0.05$ versus sham. AU, arbitrary units; GFAP, glial fibrillary acidic protein; SMA, smooth muscle actin.

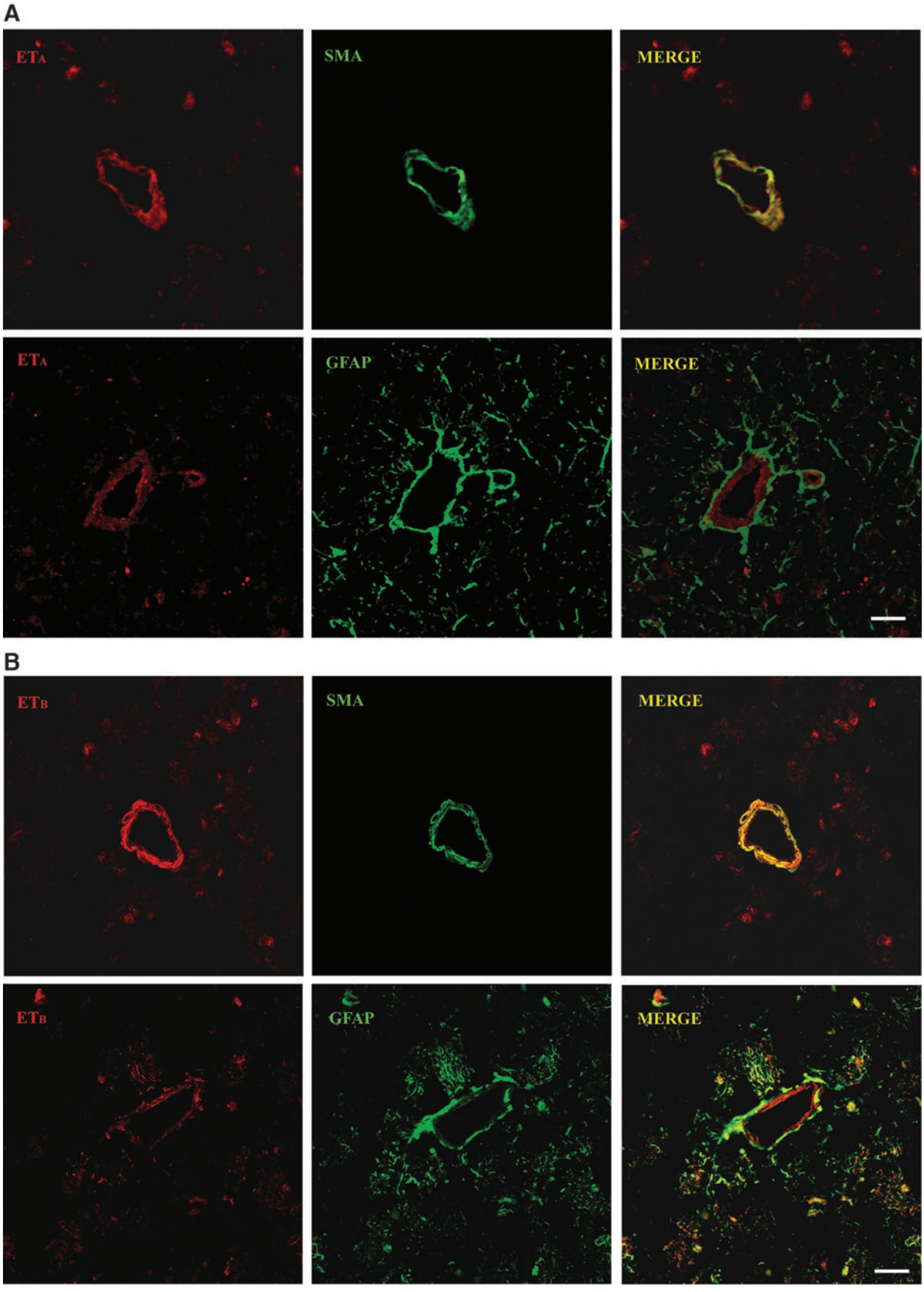
A
ETA
SMA
MERGE
ETA
GFAP
MERGE
B
ETB
SMA
MERGE
ETB
GFAP
MERGE

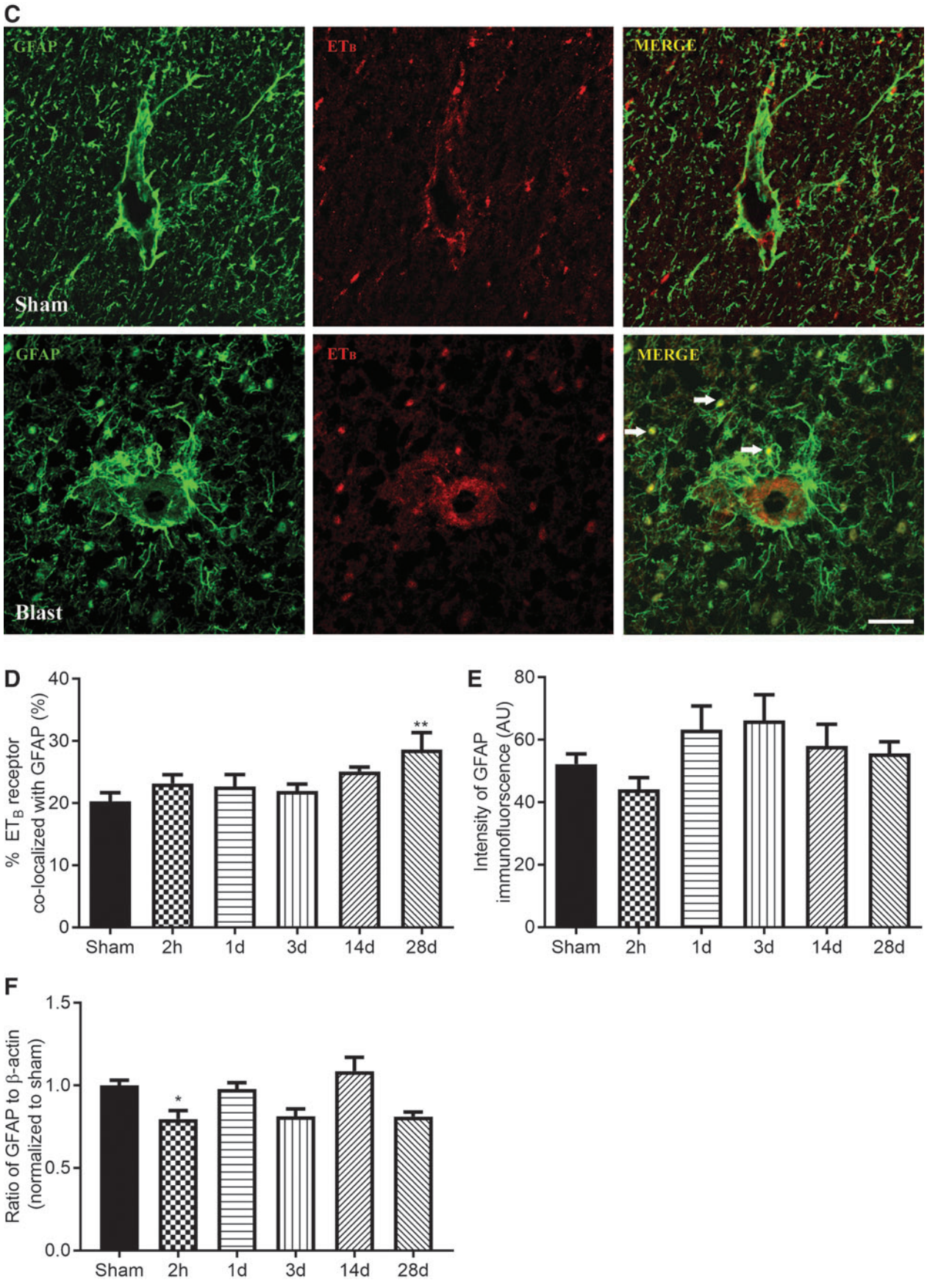

FIG 12. (Continued)

may be a result of increase in vessel tone. Blast-induced constriction of microvessels attributed to decrease in NO production and/or upregulation of receptors mediating vasoconstriction (e.g., ET_B receptor, as we show in this study) could contribute to increase in initial vessel tone. Blood pressure was not different between the blast-exposed and control groups (Table 1), and it is highly unlikely that tone differences existed between the groups because of pressure-mediated myogenic autoregulation. An increase in vessel wall thickness similar to that observed in basilar artery of blast-exposed rats[13] would increase vascular tone and lead to the observed serotonin-induced dilation; however, our data do not support this speculation.

Damage to the endothelium is another possible underlying cause of the blast-induced reversal of the serotonin effect on pial arterioles. Targeted endothelial injury that preserved vascular smooth muscle was shown to convert serotonin-induced constriction in rodent pial arterioles to dilation, indicating that endothelium injury may unmask endothelial-independent dilation.[44] Impaired CO_2-induced vasodilation after exposure to blast occurring within the same time frame as the serotonin changes lends some support to endothelial dysfunction as a contributing factor to this phenomenon. Finally, blast-induced alterations in serotonin could also contribute to reversal of the serotonin effect by changing microvascular sensitivity to serotonin. Upregulation of $5HT_{1B}$ receptor expression has been implicated in the enhancement of vasoconstriction, hypoperfusion, and the development of post-SAH vasospasm.[79,80]

It is unknown whether similar delayed changes in serotonin receptors occur after exposure to blast at the time points examined in this study, and more work is needed to characterize these potential contributing factors. Regardless of the underlying cause, our data show that exposure to blast shifts the balance of forces acting on pial arterioles stimulated with serotonin toward dilation. The precise contribution of smooth muscle versus endothelium to the altered microvascular reactivity remains to be elucidated in future studies. Given the role of the serotonergic system in the pathophysiology of migraine-type headaches,[81] the alterations in the cerebrovascular response to serotonin reported here may be of clinical relevance given that post-traumatic headaches with migraine features are reported in nearly half of blast-exposed veterans.[82]

Blast exposure induces maladaptive vascular smooth muscle changes

Phenotypic switching is a feature of several vascular pathologies, including cerebral vasospasm[17,83] and blast exposure *in vitro*[14] and *ex vivo*.[13] In our model, blast exposure was associated with a delayed loss of the contractile smooth-muscle–specific proteins (SMTH and SM-MHC) and a concomitant increase in MLC. Reduction in SMTH has been linked to loss of contractile vascular smooth muscle. Knockout mice lacking vascular SMTH show reduced vascular contractility, indicating that SMTH actively participates in smooth muscle contractility.[84] Reduction in SM-MHC occurs during ''de-differentiation'' of contractile smooth muscle cells.[85] Similar changes in both proteins have been described *in vitro* after simulated blast,[14] suggesting that exposure to blast overpressure may trigger vascular proliferation. MLC controls the activation of smooth muscle actin-myosin cross-bridge cycling. Increase in MLC is associated with hypoxia-induced vascular smooth muscle remodeling[86] and vasoconstriction post-TBI.[49] Thus, these protein changes indicate decrease in vascular contractility after blast exposure, vasoconstriction, and vascular remodeling.

Endothelial and astrocytic dysregulation after blast

ET-1 and NO are critical for healthy autoregulatory and functional control of the cerebral microcirculation and are implicated in cerebral hypoperfusion after TBI, stroke, and other cerebrovascular pathologies.[70,87–89] Blast exposure increases the sensitivity of the vascular wall to the effects of ET-1[14] and enhances arterial constriction to ET-1.[13] The temporal sequence of blast-induced events in the present study show that increase in ET-1 precedes the reduction in NOS and increase in both ET_A and ET_B expression. It has been shown that ET-1 impairs endothelial NO production and reduces endothelium-dependent vascular responses.[90] NO functions as a modulator of proliferation of vascular smooth muscle, and reduction in NO availability may result in excessive smooth muscle proliferation within the vessel wall,[91] evidence of which is also reported here. Endothelial dysregulation may be initiated by mechanical damage to structural components of endothelium caused by the overpressure and changes in shear stress,[10] leading to reduction in flow-induced NO production[92] and increase in ET-1 in the acute phase after blast exposure.

Similar to our findings after blast exposure, delayed increase in the density of ET_B has been shown in post-SAH arterial vasospasm[80] and may be associated with increased vasoconstriction as shown after ischemia.[93] The astrocytic ET-1 system is activated in different pathological conditions in which astrocytes express high levels of the endothelin receptors, mainly ET_B.[53,94] Increase in astrocytic expression of ET_B has been reported after brain injury[95,96] and may result from mechanical deformation of cellular components and increase in shear stress. In the present study, we show that the physical forces of blast overpressure trigger a delayed increase in astrocytic ET_B (by mechanisms that are yet to be determined) eliciting a ''phenotypic switch'' in astrocytes. Collectively, these changes favor vasoconstriction and increase the risk of vasospasm.

A notable finding in this study is the variable time course of the development of changes in vascular reactivity, as well as those of endothelial, vascular smooth muscle, and astrocytic proteins. Specifically, some changes occur early after blast exposure and are evident within the first few hours after exposure, such as the increase in ET-1. Other changes have a delayed manifestation and persist up to 28 days after exposure, including the increase in barium-induced vasoconstriction and serotonin-induced vasodilation. Whereas the early changes may be a direct response to the injury that result from mechanical forces, the delayed changes may result from secondary processes. A similar temporal dynamic has been shown in blast-induced disruption of BBB integrity, which also occurs in a biphasic manner (early and delayed).[97] The relationship between changes in vascular reactivity and BBB disruption after exposure to blast remains to be determined, and studies examining the interplay between these two features of blast-induced brain injury are indicated. Astrocytes are involved in regulation of both BBB and cerebral blood flow.[97–99] Considering our finding of increased expression of astrocytic ET_B receptors in blast-exposed animals, it would be important to examine the role of blast-induced changes in the perivascular astrocytes as a possible link in the dysregulation of vascular contractility and BBB integrity.

Arterial vasospasm is a prominent clinical finding in casualties exposed to explosive blast overpressures and tends to be a prolonged angiographic feature of blast-induced neurotrauma.[3] Experimentally, acute exposure to blast overpressure induces arterial vasospasm.[100] It has been suggested that exposure to blast may result in genetic changes in vascular smooth muscle cells that initiate remodeling of the vasculature and contribute to potentiation of

vasospasm.[14] Our *in vivo* studies demonstrating prolonged alterations in vasoreactivity, as well as endothelial changes and alterations in smooth muscle and astrocytic phenotype, indicate that exposure to blast impairs the microcirculation. A decline in smooth muscle contractile proteins and NO-producing enzymes, along with an increase in ET-1 and endothelin receptors (specifically on astrocytes), begin to reveal the underlying mechanisms of blast-induced dysregulation of cerebrovascular function. It is important for future studies to explore the nature of signaling among endothelial, smooth muscle, and astrocytic cells after blast exposure. The delayed incidence of functional impairment and associated vascular and astrocytic structural changes may define a therapeutic window for intervention to prevent full progression to vasospasm or other long-term vascular pathology.

Acknowledgments

The authors thank Dr. Enoch Wei for technical advice and expertise with the cranial window model. This work was supported/funded by work unit number 603115HP.3520.001.A1411. The views expressed in this article reflect the results of research conducted by of the author and do not necessarily reflect the official policy or position of the Department of the Navy, Department of Defense, nor the U.S. government. The contents of this publication are the sole responsibility of the author(s) and do not necessarily reflect the views, opinions, or policies of Uniformed Services University of the Health Sciences (USUHS), The Henry M. Jackson Foundation for the Advancement of Military Medicine, Inc., the Department of Defense (DoD), the Departments of the Army, Navy, or Air Force. Mention of trade names, commercial products, or organizations does not imply endorsement by the U.S. government. Some of the authors are military Service members [or employees of the U.S. government]. This work was prepared as part of their official duties. Title 17 USC §105 provides that copyright protection under this title is not available for any work of the U.S. government. Title 17 USC §101 defines a U.S. government work as a work prepared by a military service member or employee of the U.S. government as part of that person's official duties. The experiments reported herein were conducted in compliance with the Animal Welfare Act and per the principles set forth in the ''Guide for Care and Use of Laboratory Animals,'' Institute of Laboratory Animals Resources, National Research Council, National Academy Press, 2011.

Author Disclosure Statement

No competing financial interests exist.

References

1. Ling, G., Bandak, F., Armonda, R., Grant, G., and Ecklund, J. (2009). Explosive blast neurotrauma. J. Neurotrauma 26, 815–825.
2. Humphrey, J.D., Baek, S., and Niklason, L.E. (2007). Biochemomechanics of cerebral vasospasm and its resolution: I. A new hypothesis and theoretical framework. Ann. Biomed. Eng. 35, 1485–1497.
3. Armonda, R.A., Bell, R.S., Vo, A.H., Ling, G., DeGraba, T.J., Crandall, B., Ecklund, J., and Campbell, W.W. (2006). Wartime traumatic cerebral vasospasm recent review of combat casualties. Neurosurgery 59, 1215–1225.
4. Elder, G.A., Gama Sosa, M.A., De Gasperi, R., Stone, J.R., Dickstein, D.L., Haghighi, F., Hof, P.R., and Ahlers, S.T. (2015). Vascular and inflammatory factors in the pathophysiology of blast-induced brain injury. Front. Neurol. 6, 48.
5. Huber, B.R., Meabon, J.S., Hoffer, Z.S., Zhang, J., Hoekstra, J.G., Pagulayan, K.F., McMillan, P.J., Mayer, C.L., Banks, W.A., Kraemer, B.C., Raskind, M.A., McGavern, D.B., Peskind, E.R., and Cook, D.G. (2016). Blast exposure causes dynamic microglial/macrophage responses and microdomains of brain microvessel dysfunction. Neuroscience 319, 206–220.
6. Kawoos, U., Gu, M., Lankasky, J., McCarron, R.M., and Chavko, M. (2016). Effects of exposure to blast overpressure on intracranial pressure and blood-brain barrier permeability in a rat model. PLoS One 11, e0167510.
7. Readnower, R.D., Chavko, M., Adeeb, S., Conroy, M.D., Pauly, J.R., McCarron, R.M., and Sullivan, P.G. (2010). Increase in blood–brain barrier permeability, oxidative stress, and activated microglia in a rat model of blast-induced traumatic brain injury. J. Neurosci. Res. 88, 3530–3539.
8. Rodriguez, U.A., Zeng, Y., Deyo, D., Parsley, M.A., Hawkins, B.E., Prough, D.S., and DeWitt, D.S. (2018). Effects of mild blast traumatic brain injury on cerebral vascular, histopathological, and behavioral outcomes in rats. J. Neurotrauma 35, 375–392.
9. DeWitt, D.S., and Prough, D.S. (2008). Blast-induced brain injury and posttraumatic hypotension and hypoxemia. J. Neurotrauma 26, 877–887.
10. Hall, A.A., Mendoza, M.I., Zhou, H., Shaughness, M., Maudlin-Jeronimo, E., McCarron, R.M., and Ahlers, S.T. (2017). Repeated low intensity blast exposure is associated with damaged endothelial glycocalyx and downstream behavioral deficits. Front. Behav. Neurosci. 11, 104.
11. Gama Sosa, M.A., De Gasperi, R., Janssen, P.L., Yuk, F.J., Anazodo, P.C., Pricop, P.E., Paulino, A.J., Wicinski, B., Shaughness, M.C., Maudlin-Jeronimo, E., Hall, A.A., Dickstein, D.L., McCarron, R.M., Chavko, M., Hof, P.R., Ahlers, S.T., and Elder, G.A. (2014). Selective vulnerability of the cerebral vasculature to blast injury in a rat model of mild traumatic brain injury. Acta Neuropathol. Commun. 2, 67–67.
12. Gama Sosa, M.A., De Gasperi, R., Perez Garcia, G.S., Perez, G.M., Searcy, C., Vargas, D., Spencer, A., Janssen, P.L., Tschiffely, A.E., McCarron, R.M., Ache, B., Manoharan, R., Janssen, W.G., Tappan, S.J., Hanson, R.W., Gandy, S., Hof, P.R., Ahlers, S.T., and Elder, G.A. (2019). Low-level blast exposure disrupts gliovascular and neurovascular connections and induces a chronic vascular pathology in rat brain. Acta Neuropathol. Commun. 7, 6.
13. Toklu, H.Z., Muller-Delp, J., Yang, Z., Oktay, Ş., Sakarya, Y., Strang, K., Ghosh, P., Delp, M.D., Scarpace, P.J., Wang, K.K.W., and Tümer, N. (2015). The functional and structural changes in the basilar artery due to overpressure blast injury. J. Cereb. Blood Flow Metab. 35, 1950–1956.
14. Alford, P.W., Dabiri, B.E., Goss, J.A., Hemphill, M.A., Brigham, M.D., and Parker, K.K. (2011). Blast-induced phenotypic switching in cerebral vasospasm. Proc. Natl. Acad. Sci. U. S. A. 108, 12705–12710.
15. Brian, J.E., Faraci, F.M., and Heistad, D.D. (1996). Recent insights into the regulation of cerebral circulation. Clin. Exp. Pharmacol. Physiol. 23, 449–457.
16. Otite, F., Mink, S., Tan, C.O., Puri, A., Zamani, A.A., Mehregan, A., Chou, S., Orzell, S., Purkayastha, S., Du, R., and Sorond, F.A. (2014). Impaired cerebral autoregulation is associated with vasospasm and delayed cerebral ischemia in subarachnoid hemorrhage. Stroke 45, 677–682.
17. Nagasawa, S., Handa, H., Naruo, Y., Moritake, K., and Hayashi, K. (1982). Experimental cerebral vasospasm arterial wall mechanics and connective tissue composition. Stroke 13, 595–600.
18. Bevan, J.A., and Bevan, R.D. (1988). Arterial wall changes in chronic cerebrovasospasm: in vitro and in vivo pharmacological evidence. Annu. Rev. Pharmacol. Toxicol. 28, 311–329.
19. Borel, C.O., McKee, A., Parra, A., Haglund, M.M., Solan, A., Prabhakar, V., Sheng, H., Warner, D.S., and Niklason, L. (2003). Possible role for vascular cell proliferation in cerebral vasospasm after subarachnoid hemorrhage. Stroke 34, 427–433.
20. Ross, R. (1993). The pathogenesis of atherosclerosis: a perspective for the 1990s. Nature 362, 801–809.
21. Chavko, M., Koller, W.A., Prusaczyk, W.K., and McCarron, R.M. (2007). Measurement of blast wave by a miniature fiber optic pressure transducer in the rat brain. J. Neurosci. Methods 159, 277–281.
22. Chavko, M., Adeeb, S., Ahlers, S.T., and McCarron, R.M. (2009). Attenuation of pulmonary inflammation after exposure to blast overpressure by N-acetylcysteine amide Shock 32, 325–331.
23. Bell, R.S., Mossop, C.M., Dirks, M.S., Stephens, F.L., Mulligan, L., Ecker, R., Neal, C.J., Kumar, A., Tigno, T., and Armonda, R.A.

(2010). Early decompressive craniectomy for severe penetrating and closed head injury during wartime. Neurosurg. Focus 28, E1.
24. McKee, A.C., and Robinson, M.E. (2014). Military-related traumatic brain injury and neurodegeneration. Alzheimers Dement 10, 3 Suppl., S242–S253.
25. Levasseur, J.E., Wei, E.P., Raper, A.J., Kontos, H.A., and Patterson, J.L. (1975). Detailed description of a cranial window technique for acute and chronic experiments. Stroke 6, 308–317.
26. Rosenblum, W., and Zweifach, B. (1963). Cerebral microcirculation in the mouse brain: Spontaneous and drug-induced changes in flow and vascular diameter. Arch. Neurol. 9, 414–423.
27. Rosenblum, W.I. (1976). Pial arteriolar responses in mouse brain revisited. Stroke 7, 283–287.
28. Rebel, A., Cao, S., Kwansa, H., Doré, S., Bucci, E., and Koehler, R.C. (2006). Dependence of acetylcholine and ADP dilation of pial arterioles on heme oxygenase after transfusion of cell-free polymeric hemoglobin. Am. J. Physiol. Heart Circ. Physiol. 290, H1027–H1037.
29. Rebel, A., Ulatowski, J.A., Kwansa, H., Bucci, E., and Koehler, R.C. (2003). Cerebrovascular response to decreased hematocrit: effect of cell-free hemoglobin, plasma viscosity, and CO_2. Am. J. Physiol. Heart Circ. Physiol. 285, H1600–H1608.
30. Abutarboush, R., Scultetus, A., Arnaud, F., Auker, C., McCarron, R., and Moon-Massat, P.F. (2013). Effects of N-acetyl-L-cysteine and hyaluronic acid on HBOC-201-induced systemic and cerebral vasoconstriction in the rat. Curr. Drug Discov. Technol. 10, 315–324.
31. Moon-Massat, P., Mullah, S.H., Abutarboush, R., Saha, B.K., Pappas, G., Haque, A., Auker, C., McCarron, R.M., Arnaud, F., and Scultetus, A. (2017). Cerebral vasoactivity and oxygenation with oxygen carrier M101 in rats. J. Neurotrauma 34, 2812–2822.
32. Mullah, S.H., Abutarboush, R., Moon-Massat, P.F., Saha, B.K., Haque, A., Walker, P.B., Auker, C.R., Arnaud, F.G., McCarron, R.M., and Scultetus, A.H. (2016). Sanguinate's effect on pial arterioles in healthy rats and cerebral oxygen tension after controlled cortical impact. Microvasc. Res. 107, 83–90.
33. Abutarboush, R., Mullah, S.H., Saha, B.K., Haque, A., Walker, P.B., Aligbe, C., Pappas, G., Tran Ho, L.T.V., Arnaud, F.G., Auker, C.R., McCarron, R.M., Scultetus, A.H., and Moon-Massat, P. (2018). Brain oxygenation with a non-vasoactive perfluorocarbon emulsion in a rat model of traumatic brain injury. Microcirculation 25, e12441.
34. Abutarboush, R., Saha, B.K., Mullah, S.H., Arnaud, F.G., Haque, A., Aligbe, C., Pappas, G., Auker, C.R., McCarron, R.M., Moon-Massat, P.F., and Scultetus, A.H. (2016). Cerebral microvascular and systemic effects following intravenous administration of the perfluorocarbon emulsion Perftoran. J. Funct. Biomater. 7, E29.
35. Moon-Massat, P.F., Abutarboush, R., Pappas, G., Haque, A., Aligbe, C., Arnaud, F., Auker, C., McCarron, R., and Scultetus, A. (2014). Effects of perfluorocarbon dodecafluoropentane (NVX-108) on cerebral microvasculature in the healthy rat. Curr. Drug Discov. Technol. 11, 220–226.
36. Golech, S.A., McCarron, R.M., Chen, Y., Bembry, J., Lenz, F., Mechoulam, R., Shohami, E., and Spatz, M. (2004). Human brain endothelium: coexpression and function of vanilloid and endocannabinoid receptors. Brain Res. Mol. Brain Res. 132, 87–92.
37. Abutarboush, R., Aligbe, C., Pappas, G., Saha, B., Arnaud, F., Haque, A., Auker, C., McCarron, R., Scultetus, A., and Moon-Massat, P. (2014). Effects of the oxygen-carrying solution OxyVita C on the cerebral microcirculation and systemic blood pressures in healthy rats. J. Funct. Biomater. 5, 246–258.
38. Asano, Y., Koehler, R.C., Kawaguchi, T., and McPherson, R.W. (1997). Pial arteriolar constriction to alpha 2-adrenergic agonist dexmedetomidine in the rat. Am. J. Physiol. Heart Circ. Physiol. 272, H2547–H2556.
39. Edwards, G., Dora, K.A., Gardener, M.J., Garland, C.J., and Weston, A.H. (1998). K+ is an endothelium-derived hyperpolarizing factor in rat arteries. Nature 396, 269–272.
40. Ko, E.A., Han, J., Jung, I.D., and Park, W.S. (2008). Physiological roles of K+ channels in vascular smooth muscle cells. J. Smooth Muscle Res. 44, 65–81.
41. Marrelli, S.P., Johnson, T.D., Khorovets, A., Childres, W.F., and Bryan, R.M. (1998). Altered function of inward rectifier potassium channels in cerebrovascular smooth muscle after ischemia/reperfusion. Stroke 29, 1469–1474.
42. Johnson, T.D., Marrelli, S.P., Steenberg, M.L., Childres, W.F., and Bryan, R.M., Jr. (1998). Inward rectifier potassium channels in the rat middle cerebral artery. Am. J. Physiol. 274, R541–R547.
43. Rosenblum, W.I. (1986). Endothelial dependent relaxation demonstrated in vivo in cerebral arterioles. Stroke 17, 494–497.
44. Rosenblum, W.I., and Nelson, G.H. (1988). Endothelium-dependent constriction demonstrated in vivo in mouse cerebral arterioles. Circ. Res. 63, 837–843.
45. Rosenblum, W.I., and Nelson, G.H. (1990). Tone regulates opposing endothelium-dependent and -independent forces: resistance brain vessels in vivo. Am. J. Physiol. Heart Circ. Physiol. 259, H243–H247.
46. Harper, A.M. (1966). Autoregulation of cerebral blood flow: influence of the arterial blood pressure on the blood flow through the cerebral cortex. J. Neurol. Neurosurg. Psychiatry 29, 398–403.
47. MacKenzie, E.T., Strandgaard, S., Graham, D.I., Jones, J.V., Harper, A.M., and Farrar, J.K. (1976). Effects of acutely induced hypertension in cats on pial arteriolar caliber, local cerebral blood flow, and the blood-brain barrier. Circ. Res. 39, 33–41.
48. Baumbach, G.L., and Heistad, D.D. (1988). Cerebral circulation in chronic arterial hypertension. Hypertension 12, 89–95.
49. Kreipke, C.W., Morgan, R., Roberts, G., Bagchi, M., and Rafols, J.A. (2007). Calponin phosphorylation in cerebral cortex microvessels mediates sustained vasoconstriction after brain trauma. Neurol. Res. 29, 369–374.
50. Kim, I., Leinweber, B., Morgalla, M., Butler, W., Seto, M., Sasaki, Y., Peterson, J., and Morgan, K. (2000). Thin and thick filament regulation of contractility in experimental cerebral vasospasm. Neurosurgery 46, 440–447.
51. Sato, M., Tani, E., Fujikawa, H., and Kaibuchi, K. (2000). Involvement of rho-kinase-mediated phosphorylation of myosin light chain in enhancement of cerebral vasospasm. Circ. Res. 87, 195–200.
52. Logsdon, A.F., Lucke-Wold, B.P., Nguyen, L., Matsumoto, R.R., Turner, R.C., Rosen, C.L., and Huber, J.D. (2016). Salubrinal reduces oxidative stress, neuroinflammation and impulsive-like behavior in a rodent model of traumatic brain injury. Brain Res. 1643, 140–151.
53. Kallakuri, S., Kreipke, C.W., Schafer, P.C., Schafer, S.M., and Rafols, J.A. (2010). Brain cellular localization of endothelin receptors A and B in a rodent model of diffuse traumatic brain injury. Neuroscience 168, 820–830.
54. Wei, E.P., Hamm, R.J., Baranova, A.I., and Povlishock, J.T. (2009). The long-term microvascular and behavioral consequences of experimental traumatic brain injury after hypothermic intervention. J. Neurotrauma 26, 527–537.
55. Kontos, H.A., Wei, E.P., and Povlishock, J.T. (1981). Pathophysiology of vascular consequences of experimental concussive brain injury. Trans. Am. Clin. and Climatol. Assoc. 92, 111–121.
56. Faraci, F.M., Breese, K.R., and Heistad, D.D. (1994). Cerebral vasodilation during hypercapnia. Role of glibenclamide-sensitive potassium channels and nitricoxide. Stroke 25, 1679–1683.
57. Irikura, K., Huang, P.L., Ma, J., Lee, W.S., Dalkara, T., Fishman, M.C., Dawson, T.M., Snyder, S.H., and Moskowitz, M.A. (1995). Cerebrovascular alterations in mice lacking neuronal nitric oxide synthase gene expression. Proc. Natl. Acad. Sci. U. S. A. 92, 6823–6827.
58. Xu, H.-L., Ye, S., Baughman, V.L., Feinstein, D.L., and Pelligrino, D.A. (2005). The role of the glia limitans in ADP-induced pial arteriolar relaxation in intact and ovariectomized female rats. Am. J. Physiol. Heart Circ. Physiol. 288, H382–H388.
59. Fieschi, C., Beduschi, A., Agnoli, A., Battistini, N., Collice, M., Prencipe, M., Risso, M., and Passero, S. (1972). Regional cerebral blood flow and intraventricular pressure in acute brain injuries. Eur. Neurol. 8, 192–199.
60. Lavi, S., Gaitini, D., Milloul, V., and Jacob, G. (2006). Impaired cerebral CO_2 vasoreactivity: association with endothelial dysfunction. Am. J. Physiol. Heart Circ. Physiol. 291, H1856–H1861.
61. Zhang, F., Sprague, S.M., Farrokhi, F., Henry, M.N., Son, M.G., and Vollmer, D.G. (2002). Reversal of attenuation of cerebrovascular reactivity to hypercapnia by a nitric oxide donor after controlled cortical impact in a rat model of traumatic brain injury. J. Neurosurg. 97, 963–969.
62. Zimmermann, C.M., and Haberl, R.L. (2003). L-arginine improves diminished cerebral CO_2 reactivity in patients. Stroke 34, 643–647.
63. Wei, E.P., Kontos, H.A., and Patterson, J.L.J. (1980). Dependence of pial arteriolar response to hypercapnia on vessel size. Am. J. Physiol. 238, 697–703.

64. Rebel, A., Ulatowski, J.A., Kwansa, H., Bucci, E., and Koehler, R.C. (2003). Cerebrovascular response to decreased hematocrit: effect of cell-free hemoglobin, plasma viscosity, and CO_2. Am. J. Physiol. Heart Circ. Physiol. 285, H1600–H1608.
65. de Wit, C., Jahrbeck, B., Schäfer, C., Bolz, S.-S., and Pohl, U. (1998). Nitric oxide opposes myogenic pressure responses predominantly in large arterioles in vivo. Hypertension 31, 787–794.
66. Pohl, U., and de Wit, C. (1999). A unique role of NO in the control of blood flow. News Physiol. Sci. 14, 74–80.
67. Nakahata, K., Kinoshita, H., Hirano, Y., Kimoto, Y., Iranami, H., and Hatano, Y. (2003). Mild hypercapnia induces vasodilation via adenosine triphosphate-sensitive K+ channels in parenchymal microvessels of the rat cerebral cortex. Anesthesiology 99, 1333–1339.
68. Horiuchi, T., Dietrich, H.H., Hongo, K., Goto, T., and Dacey, R.G.J. (2002). Role of endothelial nitric oxide and smooth muscle potassium channels in cerebral arteriolar dilation in response to acidosis. Stroke 33, 844–849.
69. Lindauer, U., Vogt, J., Schuh-Hofer, S., Dreier, J.P., and Dirnagl, U. (2003). Cerebrovascular vasodilation to extraluminal acidosis occurs via combined activation of ATP-sensitive and Ca2+-activated potassium channels. J. Cereb. Blood Flow Metab. 23, 1227–1238.
70. Petrov, T., Steiner, J., Braun, B., and Rafols, J.A. (2002). Sources of endothelin-1 in hippocampus and cortex following traumatic brain injury. Neuroscience 115, 275–283.
71. Karkanis, T., Li, S., Pickering, J.G., and Sims, S.M. (2003). Plasticity of KIR channels in human smooth muscle cells from internal thoracic artery. Am. J. Physiol. Heart Circ. Physiol. 284, H2325–H2334.
72. Bir, C., VandeVord, P., Shen, Y., Raza, W., and Haacke, E.M. (2012). Effects of variable blast pressures on blood flow and oxygen saturation in rat brain as evidenced using MRI. Magn. Reson. Imaging 30, 527–534.
73. Koide, M., Bonev, A.D., Nelson, M.T., and Wellman, G.C. (2013). Subarachnoid blood converts neurally evoked vasodilation to vasoconstriction in rat brain cortex. Acta Neurochir. Suppl. 115, 167–171.
74. Ellison, M.D., Erb, D.E., Kontos, H.A., and Povlishock, J.T. (1989). Recovery of impaired endothelium-dependent relaxation after fluid-percussion brain injury in cats. Stroke 20, 911–917.
75. Raynor, R.B., McMurtry, J.G., and Pool, J.L. (1961). Cerebrovascular effects of topically applied serotonin in the cat. Neurology 11, 190–195.
76. Bell, W.H. III, Sundt, T.M., Jr., and Nofzinger, J.D. (1967). The response of cortical vessels to serotonin in experimental cerebral infarction. J. Neurosurg. 26, 203–212.
77. Harper, A.M., and MacKenzie, E.T. (1977). Effects of 5-hydrooxytryptamine on pial arteriolar calibre in anaesthetized cats. J. Physiol. 271, 735–746.
78. Edvinsson, L., Hardebo, J.E., MacKenzie, E.T., and Stewart, M. (1977). Dual action of serotonin on pial arterioles in situ and the effect of propranolol on the response. Blood Vessels 14, 366–371.
79. Larsen, C., Povlsen, G., Rasmussen, M., and Edvinsson, L. (2010). MEK1/2 inhibition improves neurological outcome and abolishes cerebrovascular ETB and 5-HT1B receptor upregulation after subarachnoid hemorrhage in the rat. J Neurosurg 114, 1143–1153.
80. Edvinsson, L.I.H., and Povlsen, G.K. (2011). Vascular plasticity in cerebrovascular disorders. J. Cereb. Blood Flow Metab. 31, 1554–1571.
81. Goadsby, P.J., Holland, P.R., Martins-Oliveira, M., Hoffmann, J., Schankin, C., and Akerman, S. (2017). Pathophysiology of migraine: a disorder of sensory processing. Physiol. Rev. 97, 553–622.
82. Finkel, A.G., Yerry, J.A., Klaric, J.S., Ivins, B.J., Scher, A., and Choi, Y.S. (2017). Headache in military service members with a history of mild traumatic brain injury: a cohort study of diagnosis and classification. Cephalalgia 37, 548–559.
83. Tani, E. (2002). Molecular mechanisms involved in development of cerebral vasospasm. Neurosurg. Focus 12, 1–8.
84. Rensen, S.S., Niessen, P.M., van Deursen, J.M., Janssen, B.J., Heijman, E., Hermeling, E., Meens, M., Lie, N., Gijbels, M.J., Strijkers, G.J., Doevendans, P.A., Hofker, M.H., De Mey, J.G., and van Eys, G.J. (2008). Smoothelin-B deficiency results in reduced arterial contractility, hypertension, and cardiac hypertrophy in mice. Circulation 118, 828–836.
85. Davis-Dusenbery, B.N., Wu, C., and Hata, A. (2011). Micromanaging vascular smooth muscle cell differentiation and phenotypic modulation. Arterioscler. Thromb. Vasc. Biol. 31, 2370–2377.
86. Adeoye, O.O., Butler, S.M., Hubbell, M.C., Semotiuk, A., Williams, J.M., and Pearce, W.J. (2013). Contribution of increased VEGF receptors to hypoxic changes in fetal ovine carotid artery contractile proteins. Am. J. Physiol. Cell Physiol. 304, C656–C665.
87. Mayhan, W.G., Faraci, F.M., and Heistad, D.D. (1987). Impairment of endothelium-dependent responses of cerebral arterioles in chronic hypertension. Am. J. Physiol. 253, 6 Pt. 2, H1435–H1440.
88. Onoda, K., Ono, S., Ogihara, K., Shiota, T., Asari, S., Ohmoto, T., and Ninomiya, Y. (1996). Inhibition of vascular contraction by intracisternal administration of preproendothelin-1 mRNA antisense oligoDNA in a rat experimental vasospasm model. J. Neurosurg. 85, 846–852.
89. Lampl, Y., Fleminger, G., Gilad, R., Galron, R., Sarova-Pinhas, I., and Sokolovsky, M. (1997). Endothelin in cerebrospinal fluid and plasma of patients in the early stage of ischemic stroke. Stroke 28, 1951–1955.
90. Faraco, G., Moraga, A., Moore, J., Anrather, J., Pickel, V.M., and Iadecola, C. (2013). Circulating endothelin-1 alters critical mechanisms regulating the cerebral microcirculation. Hypertension 62, 759–766.
91. Garg, U.C., and Hassid, A. (1989). Nitric oxide-generating vasodilators and 8-bromo-cyclic guanosine monophosphate inhibit mitogenesis and proliferation of cultured rat vascular smooth muscle cells. J. Clin. Invest. 83, 1774–1777.
92. Yen, W., Cai, B., Yang, J., Zhang, L., Zeng, M., Tarbell, J.M., and Fu, B.M. (2015). Endothelial surface glycocalyx can regulate flow-induced nitric oxide production in microvessels in vivo. PloS One 10, e0117133.
93. Cipolla, M.J., Sweet, J.G., Gokina, N.I., White, S.L., and Nelson, M.T. (2013). Mechanisms of enhanced basal tone of brain parenchymal arterioles during early postischemic reperfusion: role of ET-1-induced peroxynitrite generation. J. Cereb. Blood Flow Metab. 33, 1486–1492.
94. Hostenbach, S., D'haeseleer, M., Kooijman, R., and De Keyser, J. (2016). The pathophysiological role of astrocytic endothelin-1. Prog. Neurobiol. 144, 88–102.
95. Rogers, S.D., Demaster, E., Catton, M., Ghilardi, J.R., Levin, L.A., Maggio, J.E., and Mantyh, P.W. (1997). Expression of endothelin-B receptors by glia in vivo is increased after CNS injury in rats, rabbits, and humans. Exp. Neurol. 145, 180–195.
96. Sirén, A., Knerlich, F., Schilling, L., Kamrowski-Kruck, H., Hahn, A., and Ehrenreich, H. (2000). Differential glial and vascular expression of endothelins and their receptors in rat brain after neurotrauma. Neurochem. Res. 25, 957–969.
97. Logsdon, A.F., Meabon, J.S., Cline, M.M., Bullock, K.M., Raskind, M.A., Peskind, E.R., Banks, W.A., and Cook, D.G. (2018). Blast exposure elicits blood-brain barrier disruption and repair mediated by tight junction integrity and nitric oxide dependent processes. Sci. Rep. 8, 11344.
98. Iadecola, C., and Nedergaard, M. (2007). Glial regulation of the cerebral microvasculature. Nat. Neurosci. 10, 1369–1376.
99. Ezan, P., André, P., Cisternino, S., Saubaméa, B., Boulay, A.-C., Doutremer, S., Thomas, M.-A., Quenech'du, N., Giaume, C., and Cohen-Salmon, M. (2012). Deletion of astroglial connexins weakens the blood–brain barrier. J Cereb Blood Flow Metab 32, 457–1467.
100. Bauman, R.A., Ling, G., Tong, L., Januszkiewicz, A., Agoston, D., Delanerolle, N., Kim, Y., Ritzel, D., Bell, R., Ecklund, J., Armonda, R., Bandak, F., and Parks, S. (2009). An introductory characterization of a combat-casualty-care relevant swine model of closed head injury resulting from exposure to explosive blast. J. Neurotrauma 26, 841–860.

Address correspondence to:
Rania Abutarboush, PhD
Naval Medical Research Center
503 Robert Grant Avenue
Silver Spring, MD 20910

E-mail: rania.abutarboush.ctr@mail.mil